Construction and Building Materials 426 (2024) 136078

Contents lists available at ScienceDirect

Construction and Building Materials

journal homepage: www.elsevier.com/locate/conbuildmat

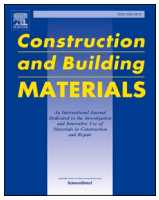

Characterizing boron-enhanced one-part alkaline-activated mortars: Mechanical properties, microstructure and environmental impacts

Ezgi Örklemez [a,*], Serhan İlkentapar [b], Ugur Durak [b], Sedat Gülçimen [c], Niğmet Uzal [c], Burak Uzal [c], Okan Karahan [b], Cengiz Duran Atiş [b]

[a] Graduate School of Natural and Applied Science, Erciyes University, Kayseri 38280, Türkiye
[b] Civil Engineering Department, Erciyes University, Kayseri 38280, Türkiye
[c] Civil Engineering Department, Abdullah Gül University, Kayseri 38080, Türkiye

ARTICLE INFO

Keywords:
Alkali-activated system
Slag
Boron refined product
Life cycle assessment

ABSTRACT

Since alkali activators negatively effect the environmental impact assessment, it is necessary to develop the alternative activators from natural sources with low environmental impact. Therefore, in this study, the usage of boron refined products colemanite, ulexite and boron pentahydrate as activators in slag-based alkali-activated mortar systems was investigated in detail. Flexural and compressive strength tests, isothermal calorimetry measurement, thermogravimetric and differential thermal analysis, inductively coupled plasma mass spectrometry analysis, field emission scanning electron microscopy, and energy dispersive analysis and elemental mapping and X-ray diffraction analysis were carried out on the samples. In addition, sample production was subjected to life cycle analysis (LCA) with a cradle-to-gate approach using two different transportation scenarios. According to the results obtained, it was determined that colemanite, ulexite and boron penta hydrate, when used in optimum proportions, had a positive effect on strength (up to increase 40% compressive strength by 20% ulexite replacement) and could be used as an activator in slag-based alkali-activated systems. The positive results obtained in strength as a result of using boron-refined products are also supported by other test results conducted within the scope of the study. Furthermore, according to the LCA results, it was observed that there was a significant decrease in global warming potential with the substitution of 20% colemanite, ulexite or boron pentahydrate as activators, not only compared to the reference sample but also traditional cementitious systems.

1. Introduction

Due to increasing urbanization, it is estimated that approximately 68% of the world's population will live in urban centers by 2050. According to 2018 data, approximately 36% of the energy used worldwide is used in the construction and construction sector. Cement, which is widely used particularly in the construction industry, is a material that requires high energy consumption during its production. In addition, cement production is held responsible for approximately 8% of the CO_2 gas released into the atmosphere in the world [1–3].

Alkali-activated binders can be produced from materials obtained as an industrial waste by-product or from natural materials. The materials that form this binding structure contain alumina (Al_2O_3), silica (SiO_2) and calcium oxide (CaO); These are mineral additives such as fly ash, blast furnace slag, silica fume, metakaolin, rice husk ash, etc., which are also used in the concrete industry [4–6]. These binding materials can react with alkaline activators (NaOH, Na_2SiO_3, KOH, $Ca(OH)_2$, etc.) at appropriate curing conditions to form alkali-activated binder systems. The use of this new binder reduces cement-derived CO_2 and contributes to the production of more environmentally friendly and sustainable building materials by enabling the use of industrial by-product materials [7–11].

Alkali-activated binders and geopolymer binders can be produced in two different ways, by two-part and one-part mixture methods. In the two-part mixture method, the binder is mixed with a previously prepared activator solution, while in the one-part mixture method, water is added directly to the dry mixture consisting of the binder and solid activator. Highly corrosive and viscous alkali solutions are difficult to transport and store in the two-part mixture method. Therefore, the two-part mixture of alkali-activated systems greatly affects and limits rapid production. On the other hand, the one-part mixture method, which is easier to produce, has been investigated more recently as it provides the

* Corresponding author.
E-mail address: orklemezezgi@gmail.com (E. Örklemez).

https://doi.org/10.1016/j.conbuildmat.2024.136078
Received 6 February 2024; Received in revised form 20 March 2024; Accepted 29 March 2024
Available online 6 April 2024

feasibility of large-scale applications [12–16]. The binders used in one-part mixtures or two-part mixtures are generally the same (e.g. blast furnace slag, fly ash, silica fume, metakaolin, etc.). Na_2SiO_3, NaOH, Na_2CO_3 CaO and CaOH are used separately or combined as solid activators in one-part mixtures [5,13,17].

Studies have been carried out in the literature to produce new types of alkali-activated and geopolymer binders. Three different types of materials have been introduced by replacing alumina or silica with new types of particles, thus, aluminogermanate geopolymers, phosphoric acid-based geopolymers, and boroaluminosilicate geopolymers are formed [18–20]. The emergence of boroaluminosilicate geopolymer aimed to reduce cost and environmental impacts. Borax has been replaced by sodium silicate as a new alkaline activator. Replacing aluminum atoms in conventional aluminosilicate geopolymers with boron ions formed the structure of boroaluminosilicate geopolymer and promoted gel formation [18,21–25]. Alkaline-activated binders, known for their eco-friendly characteristics are theorized to contribute to their lower environmental impact compared to conventional silicate-based binders. Regardless of these claims, the specific environmental advantages attributed to borax utilization as an activator in this particular context remain unquantified, due to the absence of life cycle assessment (LCA) studies in this field. This study intends to fill this notable gap by focusing on the LCA of alkaline-activated binders, particularly examining the role and impact of borax in enhancing their environmental sustainability.

LCA is a critical methodology utilized in the construction industry to evaluate and quantify the environmental impacts of materials throughout their entire life cycle, covering extraction to end-of-life. The significance of LCA data is significantly noticeable in the development of Environmental Product Declarations (EPDs), which rely heavily on this information. The significance of incorporating LCA into EPDs and adhering to ISO guidelines is further highlighted by the fact that it promotes sustainable practices in the construction industry. Previous studies that utilized LCA have shown that alkali-activated and geopolymer systems exhibit superior environmental performance in comparison to conventional cementitious systems. Furthermore, these systems quantify greenhouse gas emissions by 28–80% less than those of the conventional systems [26–32]. In this regard, Moraes et. al. (2023) investigated the long-term resistance to chemical attacks and performed LCA on alkali-activated binder incorporating sugar cane straw ash. The samples were compared to one that exclusively consisted of blast furnace slag and another that solely included Portland cement. LCA results showed that the alkali-activated binder with sugar cane straw ash had a 28% lower global warming potential (GWP) compared to the Portland cement sample [33]. Furthermore, Robayo-Salazar et. al (2018) performed LCA to evaluate the environmental efficiency of alkali-activated binary concrete, which was produced by combining natural volcanic pozzolan from Colombia (70%) and granulated blast furnace slag (30%) with normal Portland cement concrete. According to the researchers, the global warming potential (GWP) of alkali-activated binary concrete is 44.7% less than that of standard Portland cement concrete [31].

Although alkali-activated and geopolymer materials are environmentally friendly and sustainable; studies conducted in recent years have found that the most negative environmental impact during the production of these binders is caused by the alkali activators used. For this reason, researchers have begun to evaluate alternative activators for the production of sustainable building materials with adequate performance in terms of high mechanical and durability aspects and low environmental impacts [32,34,35]. For instance, Gopalakrishna and Dinakar (2024) conducted a study to examine the impact of alkaline activator content on the mechanical and microstructural features, as well as the environmental performance, of geopolymer mortar. The researchers applied the LCA methodology in their study and found that the geopolymer binder exhibited much lower environmental impacts of embodied energy (EE) and GWP compared to the conventional Portland cement-based mortar, with reductions of 94% and 97% respectively [36]. Furthermore, a study on the environmental impacts of geopolymer including fly ash and silica fume has been conducted by Bajpai et al. (2020). According to their outcomes of LCA, the primary contributors to environmental impacts in geopolymer and cement concrete, are alkaline activators and cement, respectively. In comparison to conventional cement concrete, geopolymer concrete containing fly ash and silica fume exhibits 69% lower environmental impact in terms of GWP [37].

According to LCA studies, another important environmental impact in alkaline-activated materials arises from the curing method. Room curing, due to its lower temperature requirements, results in less energy usage during production. This makes it a more environmentally friendly and sustainable method of production. Specifically, binders that are activated by blast furnace slag and alkali can increase their strength through room temperature curing, more than fly ash-based geopolymer systems. This approach enables the efficient production of powdered alkali activators and blast furnace slag through a single-step mixing process. The reactive powder mixture consisting of blast furnace slag and solid activator is triggered by the addition of water, forming the binder system and providing strength [14,32,38,39].

When the environmental effects of alkali-activated systems are examined, it is observed that the most negative effect is caused by activators (Na_2SiO_3, NaOH etc.). Therefore, it is necessary to develop alternative activators to the activators used in alkaline systems. There are some studies in the literature where boron products (borax) are used as activators. However, there is no detailed study on borax, colemanite and ulexite. Therefore, in this study, the usability of borax, colemanite and ulexite, which are boron refined products, as alkaline activators in slag-based alkali systems were investigated within the scope of strength, microstructure and environmental impact assessment. In summary, the main purpose of this study is to develop alternatives to alkaline activators that have a significant environmental impact in alkaline-activated binders, which are claimed to be environmentally friendly and sustainable. In the study, blast furnace slag-based mortars were activated with a combined activator consisting of sodium metasilicate and boron-refined products. 26 different mortars were produced by substituting 10%, 20%, 30% and 40% of the activator amounts in two different reference mortar groups containing 6% and 8% Na^+ with refined boron products (colemanite, ulexite and boron pentahydrate). While this substitution process was achieved with borax in the studies published in literature [21–24], in this work, alternatives to alkaline activators were developed with three different boron refined products: colemanite, ulexite and boron pentahydrate. In addition, in this study, the environmental impacts of mortars produced with boron combined activators, traditional alkali-activated mortars and cementitious mortars were examined using the life cycle analysis methodology. Moreover, the one-part mixture method was preferred in the study, to provide more suitable for commercial use. Also, it was aimed to ensure energy efficiency by subjecting the mortars to room cure. The flexural and compressive strengths of all mortar samples produced in the study were measured at 3, 7, and 28 days. Then, FESEM, EDX, Mapping, XRD, TGA, Isothermal calorimetry and ICP analyses were performed on the samples selected according to the strength results. In addition, LCA was carried out on the mixtures that provided optimum strength results.

2. Materials and methods

2.1. Blast furnace slag

Blast furnace slag with a specific gravity of 2.85 g/cm^3, obtained from Kayseri Çimsa company, was used in the study. The chemical properties of the blast furnace slag are given in Table 1. Also, the FESEM and XRD patterns of blast furnace slag are provided in Fig. 1.

Table 1
Chemical compositions of blast furnace slag (%).

Oxide (%)	SiO_2	CaO	Al_2O_3	Fe_2O_3	K_2O	MgO	Na_2O	TiO_2	SO_3	MnO	Diğer	LOI
Blast Furnace Slag	39.4	35.21	10.55	1.45	0.77	6.91	0.22	0.45	1.02	1.56	0.26	2.2

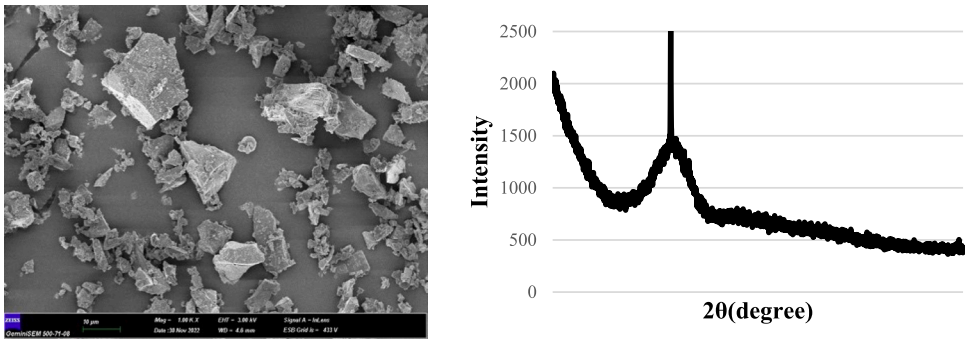

Fig. 1. FESEM images (1000x) and XRD of blast furnace slag.

2.2. Sand, water and activator

CEN standard RILEM sand complying with TS EN 196–1 [40] was used as fine aggregate in the experiments. The dry specific gravity of the sand is 2.63 g/cm^3 and the water absorption rate is 0.5%. City tap water was used in the production of mortar mixtures. Anhydrite sodium metasilicate (Na_2SiO_3) obtained from the Silmaco company was used as an activator in the study. The chemical properties of sodium metasilicate are presented in Table 2.

2.3. Colemanite, ulexite and boron pentahydrate

Refined boron products colemanite ($2CaB_3O_3.5\ H_2O$) and ulexite ($Na_2O.2CaO.5B_2O_3.16\ H_2O$) were supplied from Eti Maden Balıkesir-Bigadiç Boron Processing Factory. Boron pentahydrate ($Na_2B_4O_7.5\ H_2O$) was obtained from Eti Maden Kırka Eskişehir Boron Processing Factory. The specific gravity of colemanite, ulexite and boron pentahydrate are 2.5 g/cm^3, 2.13 g/cm^3 and 1.82 g/cm^3, respectively. The chemical properties of boron-refined products are given in Table 3, Table 4, and FESEM, and XRD images are presented in Fig. 2.

2.4. Mix design

While producing the samples, the water/binder ratio was kept constant (0.42) for all mixtures. The sand/binder ratio was taken as 3.0 according to TS EN 196–1 [40]. A composite activator consisting of sodium metasilicate (Na_2SiO_3) and refined boron products (colemanite (C), ulexite (U) and boron pentahydrate (B)) was used as the activator. In sodium metasilicate activated slag systems, it has been observed that high strength results are obtained when activator is used in the range of 6% - 12% [41–43]. However, according to the studies [44–50], the use of activator at high rates causes serious negative environmental impacts. Therefore, in this study, it was preferred to use 6% and 8% activator ratios by avoiding the use of high activator ratios. In the reference samples (Ref-6 N and Ref-8 N), activators were used to contain 6% (group 1) and 8% (group 2) Na^+ by weight of binder, respectively.

Table 2
Chemical compositions of sodium metasilicate.

Molar ratio	$SiO_{2\%}$	Na_2O %	pH	Dry matter %	Bulk density (g/L)	Melting point (C)
1.0	47	50	>12.5	97	1.10	1089

Refined boron products were replaced with Na_2SiO_3 at the ratio of 10%, 20%, 30% and 40% in mass basis. The mixing ratios and codes of the mortars are given in Table 5. The mixture name contains activator replacement ratio, boron refined product, and group number. For example; 10 C-1 means the mixture produce with 10% colemanite replacement with activator for group 1.

2.5. Experimental program

First, blast furnace slag, Na_2SiO_3, and boron-refined products were placed in the mixing bowl. Dry particles were mixed in powder form with a spoon and water was added. Second, the mixture was mixed at slow speed for 30 seconds and 1350 g of sand was added to the mixing bowl. After continuing the mixing process at a slower speed for 60 seconds, the mixer was stopped, the mortar surrounding the mixing bowl was scraped off and collected in the middle of the bowl, and mixed at high speed for another 90 seconds. Third, fresh mortar mixtures were placed in steel molds with a dimension of 40×40×160 mm by using a vibration table. The produced samples were cured at room temperature (23±2°C) for 3, 7, and 28 days. The production stages are shown in Fig. 3.

2.5.1. Flexural and compressive strength test

Flexural and compressive strength tests were carried out on the samples after completing the curing process (3, 7, and 28 days) by TS EN 1015–11 [51]. The flexural strength test was carried out on three prismatic samples for each mixture and the flexural strength values were determined by taking their averages. Compressive strength test results were performed on six halved sample pieces obtained after the flexural strength test, and compressive strength values were determined by taking their averages.

2.5.2. Isothermal calorimetry measurement

Isothermal calorimetry was used to determine the reaction kinetics of alkali-activated paste samples. To evaluate the effects of refined boron products on the heat release of paste samples, the heat flow curve was recorded with an 8-channel isothermal calorimeter (TAM Air, TA Instruments) based on the ASTM C1679[52] standard. The water/binder ratio in the produced alkali-activated paste samples was taken as 0.42 same as the mortar. Test samples were placed in plastic molds of 2.5 cm in diameter and 6 cm in height and placed in an isothermal calorimeter and measurements were carried out. Calorimetric data were monitored for 72 hours and the corresponding integral curve was calculated.

Table 3
Chemical compositions of colemanite and ulexite (%).

Oxide (%)	B_2O_3	CaO	SiO_2	SO_4	Fe_2O_3	Al_2O_3	MgO	Na_2O	SrO	LOI	Other
Colemanite	36.57	24.82	4.45	0.5	0.06	0.32	1.89	0.5	1.04	28.85	1
Ulexite	36.63	17.08	3.98	0.2	0.02	0.24	2.2	3.2	1	34.5	0.97

Table 4
Chemical compositions of boron pentahydrate (%).

Oxide (%)	B_2O_3	Na_2O	SO_4	CI	Fe	LOI
Boron Pentahydrate	47.7	21.35	200 ppm	70 ppm	3 ppm	31.34

2.5.3. Thermogravimetric and Differential Thermal Analysis (TGA/DTA)

Thermogravimetric analysis of the samples that completed the 28-day curing process was performed with the DT-TGA device (DTG-60 H TGA, Shimadzu). The experiment was carried out with a heating rate of 10 °C/min for the temperature range from ambient temperature to 1000°C.

2.5.4. Inductively Coupled Plasma Mass Spectrometry (ICP-MS)

Inductively coupled plasma mass spectrometry (ICP–MS) is generally employed to identify the presence of the elements. Variation in the chemical composition of the mixture influences the hydration kinetics and mechanical properties of the material. To determine the variations in the chemical composition of paste, an ICP test was carried particularly on the concentration of B, Na, Ca, Al and Fe ions using an AGILENT brand 7500 A model device.

2.5.5. Field emission scanning electron microscopy (FE-SEM) -Energy Dispersive X-ray (EDX) and Elemental Mapping

FESEM imaging and EDX analyses were performed to examine the microstructural properties of the alkali-activated samples. The samples after the 28-day curing process were broken and broken surface pieces were taken from the middle parts of the sample. They were vacuum-sealed and then coated with gold-palladium to provide a conductive surface before FESEM imaging. The samples were placed in the Zeiss GeminiSEM electron microscope and microstructure examinations were performed. Additionally, EDX analyses and elemental mapping were performed in the areas selected during the FESEM analysis. For elemental mapping of the samples, the elements silicon (Si), aluminum (Al), sodium (Na), oxygen (O), boron (B) and calcium (Ca) were taken into account. The choice of elements is a result of the elemental composition of the material, consisting of slag, sodium metasilicate (Na2SiO3), and boron materials.

2.5.6. X-ray diffraction (XRD) analysis

XRD analysis was performed on 28-day-cured samples. The pieces taken from the alkali-activated samples were ground into powder and sieved below 63 microns. Then, analyses were made between 5 and 60° 2-theta angles using a Bruker AXS D8 model XRD device working with a CuKa X-ray source.

2.5.7. Life Cycle Assessment (LCA) methodology

LCA is a widely used methodology to evaluate the environmental impacts of a process, product or service throughout its lifecycle. According to ISO 14040 [28] and 14044 [53] LCA consists of four main stages: goal and scope definition, inventory analysis, impact assessment and interpretation.

2.5.7.1. Goal and scope definition. The main purpose of LCA in this study is to quantify and compare the environmental impacts of produced mixtures. In this context, the environmental impacts of cementitious (PC) mortar, control mortar (Ref-8 N), mortar mixtures containing 20% colemanite (20 C-2), ulexite (20 U-2) and boron pentahydrate (20B-2)

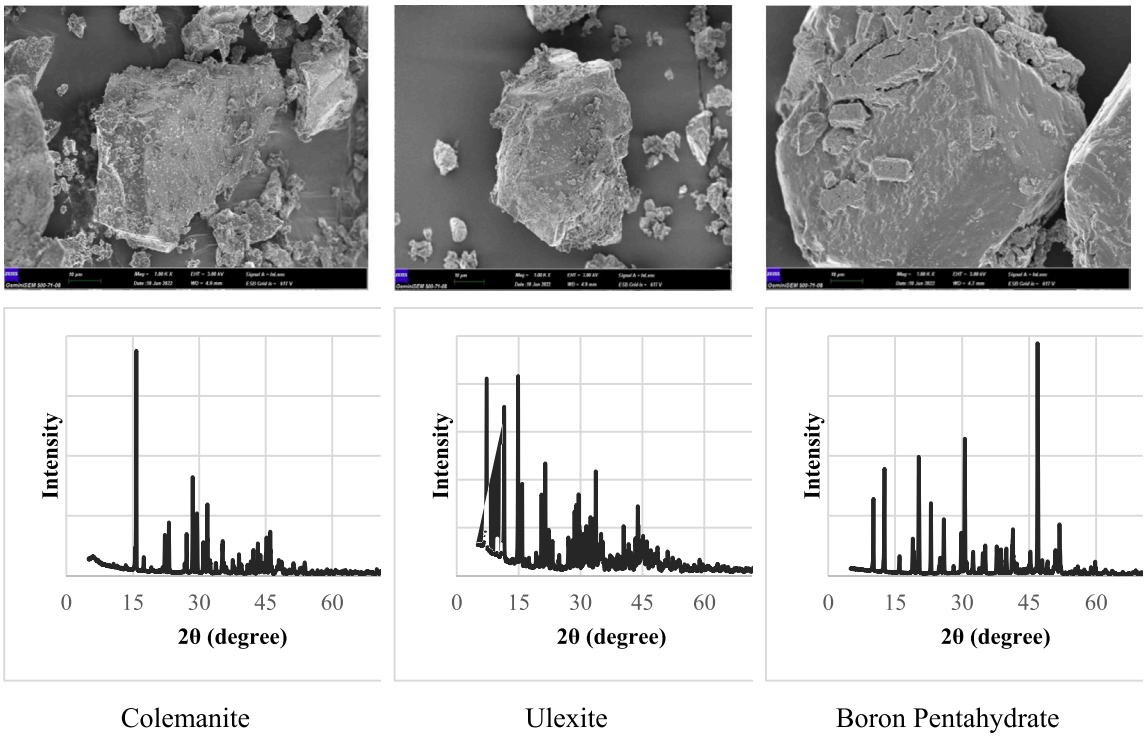

Fig. 2. FESEM images (1000x) and XRD of boron-refined product.

Table 5
Mix design of mortars.

Group	Code	Slag (g)	Sand (g)	Water (g)	Na_2SiO_3 (%)	Colemanite (%)	Ulexite (%)	Boron Pentahydrate (%)
First group	**Ref-6N**	450	1350	190	100	-	-	-
	10 C-1	450	1350	190	90	10	-	-
	20 C-1	450	1350	190	80	20	-	-
	30 C-1	450	1350	190	70	30	-	-
	40 C-1	450	1350	190	60	40	-	-
	10 U-1	450	1350	190	90	-	10	-
	20 U-1	450	1350	190	80	-	20	-
	30 U-1	450	1350	190	70	-	30	-
	40 U-1	450	1350	190	60	-	40	-
	10B-1	450	1350	190	90	-	-	10
	20B-1	450	1350	190	80	-	-	20
	30B-1	450	1350	190	70	-	-	30
	40B-1	450	1350	190	60	-	-	40
Second group	**Ref-8N**	450	1350	190	100	-	-	-
	10 C-2	450	1350	190	90	10	-	-
	20 C-2	450	1350	190	80	20	-	-
	30 C-2	450	1350	190	70	30	-	-
	40 C-2	450	1350	190	60	40	-	-
	10 U-2	450	1350	190	90	-	10	-
	20 U-2	450	1350	190	80	-	20	-
	30 U-2	450	1350	190	70	-	30	-
	40 U-2	450	1350	190	60	-	40	-
	10B-2	450	1350	190	90	-	-	10
	20B-2	450	1350	190	80	-	-	20
	30B-2	450	1350	190	70	-	-	30
	40B-2	450	1350	190	60	-	-	40

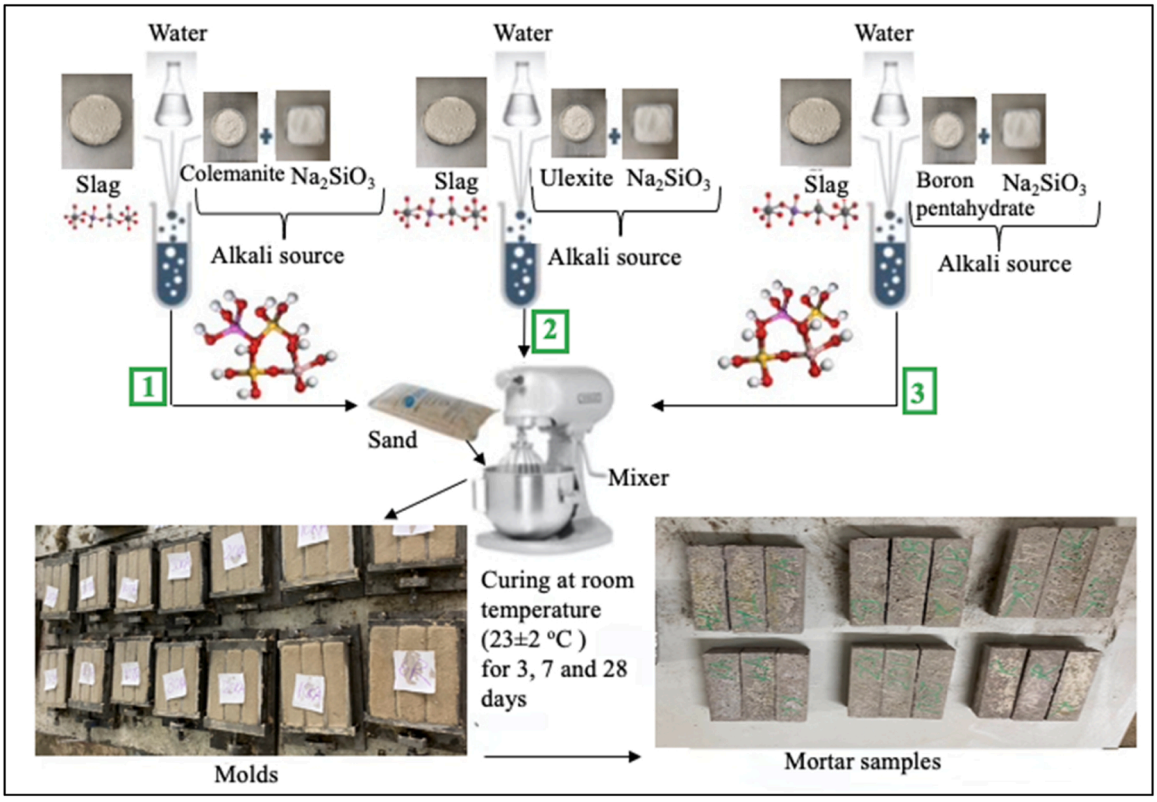

Fig. 3. Production stages of mortars.

were quantified and compared with each other. The functional unit was chosen as 1 m^3 per MPa. This study followed a cradle-to-gate approach covering life cycle stages from raw material extraction to mortar production. The system boundaries of different mortars are given in Fig. 4.

2.5.7.2. Life Cycle Inventory (LCI) analysis. LCI involves data collection and calculation to measure the inputs and outputs of materials and energy associated with a product system. The primary inventory data related to the amount of raw materials, energy consumption, and water use of mortar mixtures was adapted from laboratory-scale experimental studies. In this study, it is assumed that raw materials (Portland cement, blast furnace slag, sand, sodium metasilicate, colemanite, ulexite, and

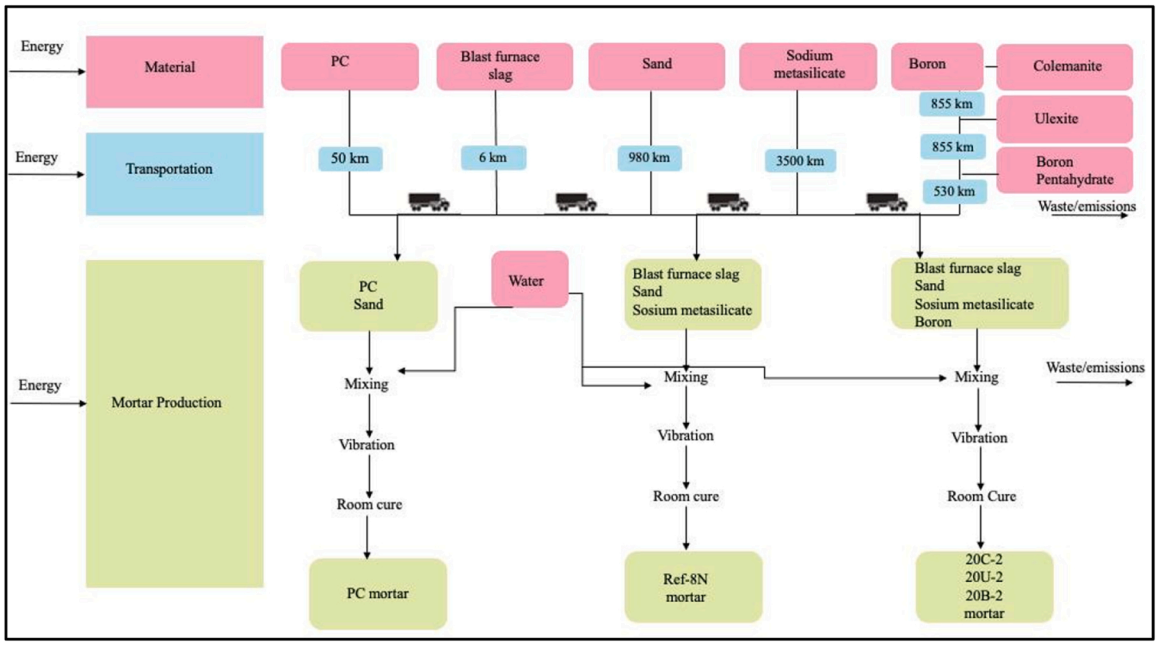

Fig. 4. The system boundaries of mortars (cradle-to-gate approach).

borax) are transported by road, with a diesel fuel truck weighing 16–32 t, complying with EURO 4 standards. Transportation distances are determined using Google Maps. Transportation distances are given in Fig. 4. Portland cement with strength class 42.5 and specific gravity 3.14 g/cm^3 and CEN standard RILEM sand were used to produce cementitious PC mortar. The secondary data for the production of raw materials, energy and transport data were retrieved from the Ecoinvent 3.9.1 database in SimaPro 9.5 software and literature search. All collected data are shown in Table S1 (see Supplementary Materials).

There are limited resources in the literature on LCI of boron mining. The inventory data for boron mining was taken from the article by Türkbay et al. (2022). Türkbay et al. obtained the data in their study by compiling it from the State Planning Organization of Turkey, Eti Mining Operations General Directorate. Borate ore (tincal, colemanite, ulexite) is mined by open pit mining method in Turkey. The ore stream is then transported to the concentrator plant and enriched by increasing the B_2O_3 grade in the mineral. Refined products are obtained from enriched ore [54].

2.5.7.3. Life Cycle Impact Assessment (LCIA). For the impact assessment of mortar production, the CML-IA baseline method was used in the SimaPro 9.5 software [55]. This method covers the following environmental impact categories: abiotic depletion (AD, kg Sb eq), abiotic depletion-fossil fuels (AD-FF, MJ), global warming potential (GWP, kg CO_2 eq), ozone depletion (ODP, kg CFC −11 eq), human toxicity (HT, kg 1,4-DB eq), freshwater aquatic ecotoxicity (FAE, kg 1,4-DB eq), marine ecotoxicity (MAE, kg 1,4-DB eq), terrestrial ecotoxicity (TE, kg 1,4-DB equivalent), photochemical oxidation (PO, kg C_2H_4 eq), acidification potential (AP, kg SO_2 equivalent), eutrophication potential (EP, PO43- eq).

3. Result and discussion

3.1. Flexural strength results

The flexural strengths of the reference mortar activated with solely Na_2SiO_3 and the slag-based mortars activated with a mixture of sodium metasilicate-refined boron products (hybrid activator with colemanite, ulexite, or borax addition) are presented in Fig. 5 and Fig. 6.

According to the 3-day flexural test results for the 6% Na^+ containing

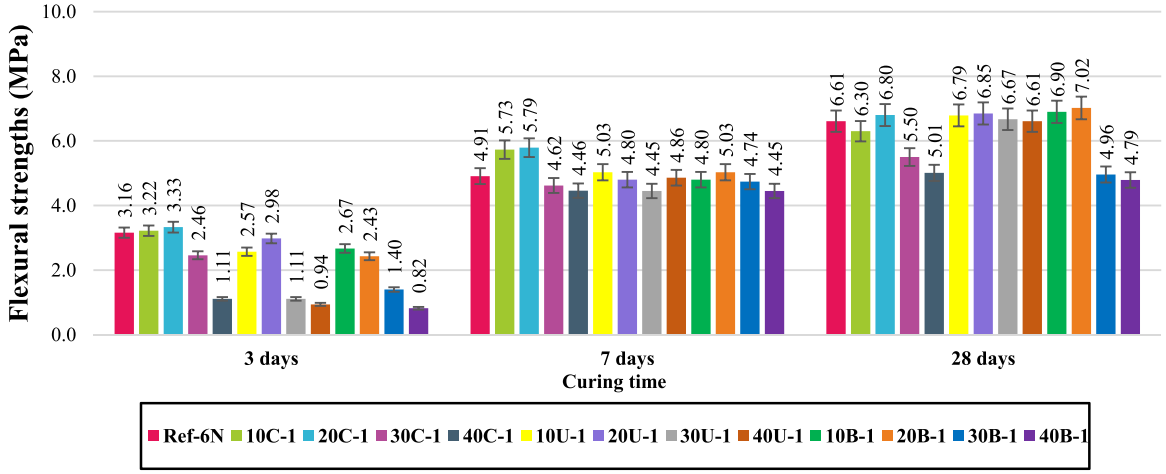

Fig. 5. Flexural strength of first-group mortars.

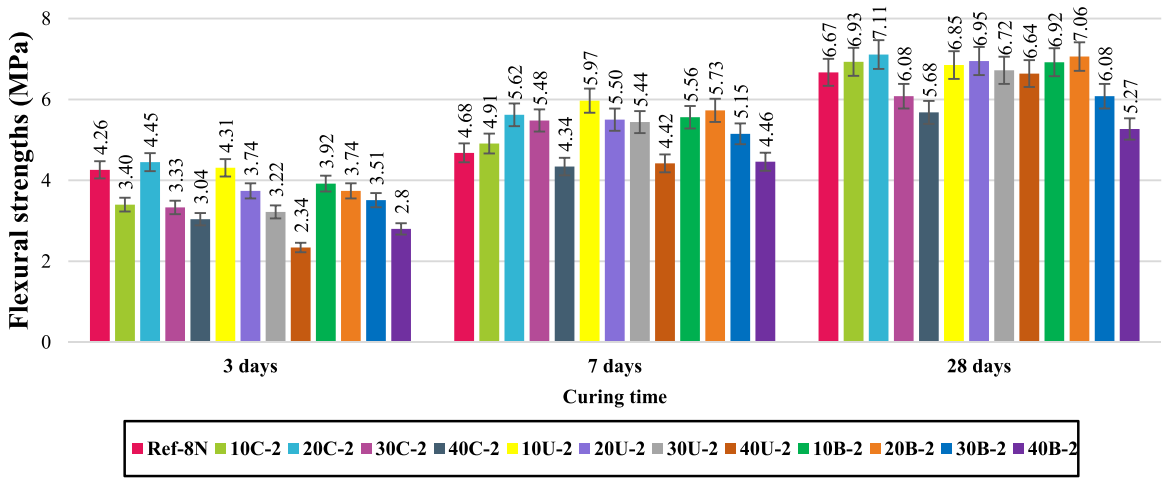

Fig. 6. Flexural strength of second-group mortars.

group, the flexural strengths of ulexite and boron pentahydrate mortars decreased compared to the reference sample at all replacement rates, while 10% and 20% colemanite replacement rates increased the flexural strengths. When the 7-day flexural strength results of the 6% Na^+ group were evaluated, increases in flexural strength were observed in mixtures containing colemanite, ulexite and boron pentahydrate for 10% and/or 20% replacement rates, compared to the reference sample.

When the 28-day flexural strength results for the 6% Na group were examined, the mixtures containing 20% colemanite, ulexite, and boron pentahydrate individually showed 3%, 4%, and 6% increases in flexural strength compared to the reference mixture, respectively. On the other hand, at all ages (3–7–28 days) the flexural strengths at 30% and 40% colemanite, ulexite and boron pentahydrate replacement rates are lower than the reference sample.

According to the 3-day flexural test results for the 8% Na^+ containing group, the flexural strengths of boron pentahydrate mortars decreased compared to the reference sample at all replacement rates, while 10% ulexite and 20% colemanite replacement rates increased the flexural strengths. When the 7-day flexural strength results of the 8% Na^+ group were evaluated, increases in flexural strength were observed in mixtures containing colemanite, ulexite, and boron pentahydrate for 10%, 20% and 30% replacement rates, compared to the reference sample.

When the 28-day flexural strength results for the 8% Na^+ group were examined, the mixtures containing 20% colemanite, ulexite and boron pentahydrate individually showed 7%, 4% and 6% increase in flexural strength compared to the reference mixture, respectively. On the other hand, at all ages (3–7–28 days) the flexural strengths at 40% colemanite, ulexite and boron pentahydrate replacement rates are lower than the reference sample.

3.2. *Compressive strength results*

The compressive strengths of the reference mortar and the slag-based mortars activated with a mixture of sodium metasilicate-refined boron products (hybrid activator with colemanite, ulexite or boron pentahydrate) are presented in Fig. 7 and Fig. 8.

The compressive strength of the specimens made with 6% Na^+, at 10% and 20% colemanite replacement ratio increased at curing times of 3, 7 and 28 days compared to the reference specimen. 30% colemanite replacement ratio decreased the compressive strength of the specimens at 3 and 7 days compared to the reference specimen, however, increased at 28 days. 40% colemanite substitution decreased the compressive strength of the specimens at all curing times (3, 7, and 28 days) in comparison to the reference specimen.

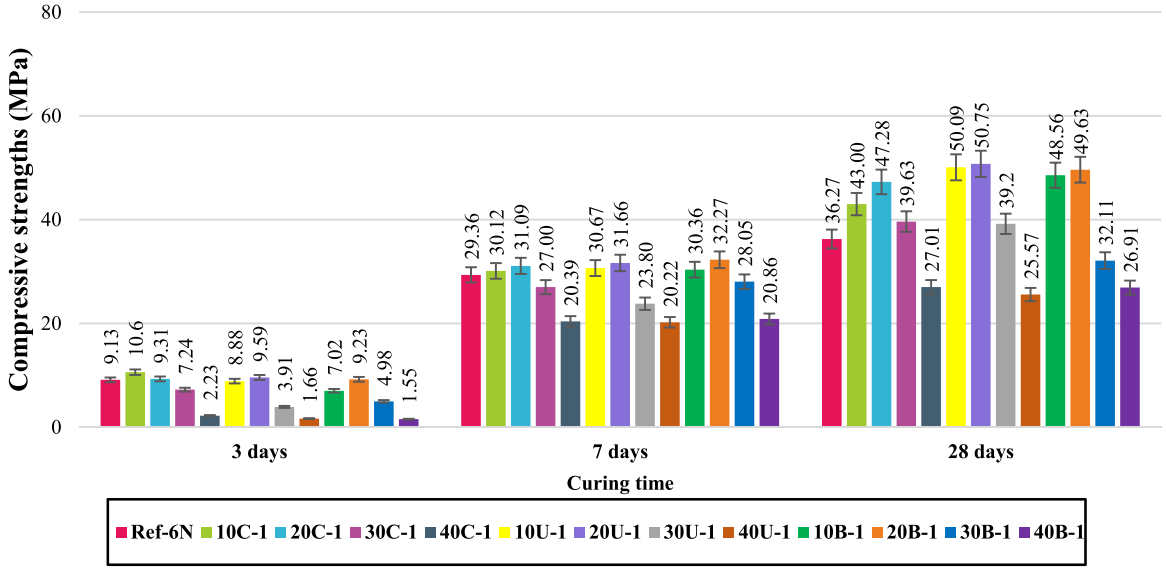

Fig. 7. Compressive strength of first group mortars.

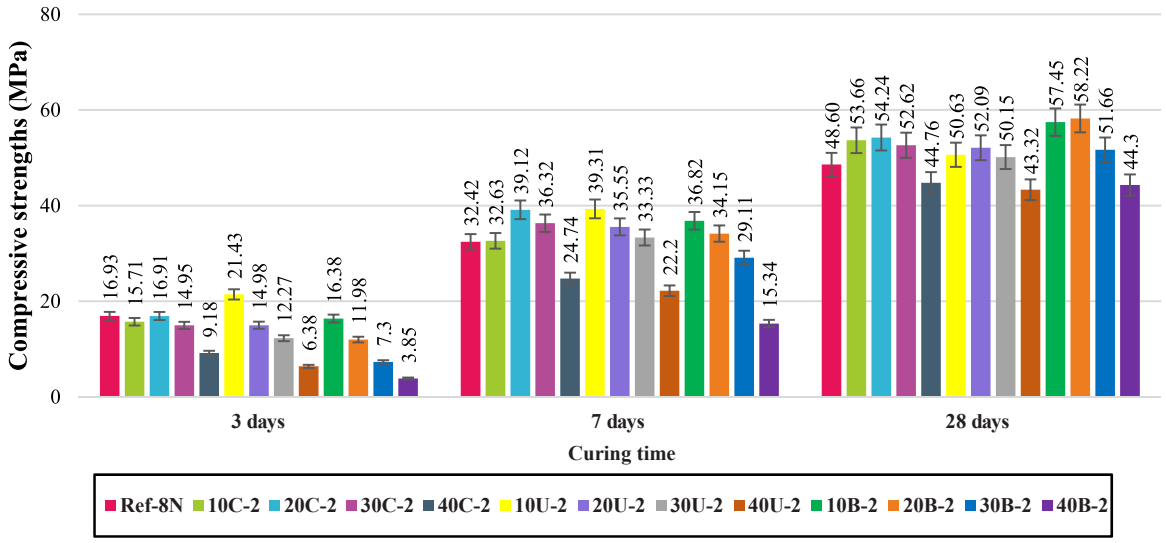

Fig. 8. Compressive strength of second group mortars.

The compressive strength of the specimens decreased at 3 days and increased at 7 and 28 days compared to the reference specimen for 10% ulexite or boron pentahydrate substitution. The compressive strength of the specimens increased at 3, 7 and 28 days compared to the reference specimen for 20% ulexite or boron pentahydrate substitution. 30% ulexite substitution decreased the compressive strengths at 3 and 7 days and increased at 28 days compared to the reference specimen. The 30% boron pentahydrate substitution decreased the compressive strength of the specimens on days 3, 7, and 28 compared to the reference specimen. 40% ulexite or boron pentahydrate substitution decreased the compressive strength on curing days 3, 7 and 28 compared to the reference specimen.

When the compressive strengths obtained were evaluated, it was seen that the highest increase in compressive strength was obtained at 28-day specimens. According to the 28-day compressive strength results, compared to the reference specimen made with 6% Na^+, the compressive strengths of mortar specimens made with 10%, 20%, and 30% colemanite substitution increased by 18%, 30%, and 9%, respectively, while a 26% decrease was determined at a 40% substitution rate.

Similarly, the compressive strengths of mortar specimens with 10%, 20%, and 30% ulexite substitution increased by 38%, 40%, and 8%, respectively, while the 40% substitution rate decreased by 30% compared to the reference specimen. The compressive strengths of mortar specimens with 10% and 20% boron pentahydrate substitution increased by 33% and 36% compared to the reference specimen, while the 30% and 40% substitution rates decreased by 12% and 26%.

According to the 28-day compressive strength results, the reference specimen with 6% Na content was 36.27 MPa, while the highest strength was obtained in mortar specimens produced with 20% ulexite substitution (50.75 MPa). The lowest compressive strength was obtained in the mortar specimens containing 40% ulexite (25.57).

The compressive strength of the specimens made with 8% Na^+, at 10%, %20, %30 and %40 colemanite replacement ratio reduced at curing times of 3 days compared to the reference specimen. 10%, %20, and %30 colemanite replacement ratio increased the compressive strength of the specimens while %40 colemanite substitution decreased the compressive strength at 7 and 28 days compared to the reference specimen.

The compressive strength of the specimens increased at all curing times (3, 7, 28 days) compared to the reference specimen for 10% ulexite substitution. %20, %30, and %40 ulexite replacement ratio decreased the compressive strength of the specimens at 3 days compared to the reference specimen. %20 and %30 ulexite replacement ratio increased the compressive strength of the specimens while %40 ulexite substitution decreased it compared to the reference specimen at 7 and 28 days.

The compressive strength of the specimens decreased at 3 days compared to the reference specimen for 10%, 20%, 30% and 40% boron pentahydrate substitution. 10% and 20% boron pentahydrate replacement ratio increased the compressive strength of the specimens while 30% and 40% boron pentahydrate substitution decreased it compared to the reference specimen at 7 days. 10%, 20%, and 30% boron pentahydrate replacement ratios increased the compressive strength of the specimens while 40% boron pentahydrate substitution decreased it compared to the reference specimen at 28 days.

According to the 28-day compressive strength results, compared to the reference specimen made with 8% Na^+, the compressive strengths of mortar specimens made with 10%, 20%, and 30% colemanite substitution increased by 10%, 12%, and 8%, respectively, while an 8% decrease was determined at a 40% substitution rate. Similarly, the compressive strengths of mortar specimens with 10%, 20%, and 30% ulexite substitution increased by 4%, 7%, and 3%, respectively, while the 40% substitution rate decreased by 11% compared to the reference specimen. The compressive strengths of mortar specimens with 10%, 20% and 30% boron pentahydrate substitution increased by 18%, 20% and 6% compared to the reference specimen, while the 40% substitution rates decreased by 9%.

According to the 28-day compressive strength results, the reference specimen with 8% Na content was 48.60 MPa, while the highest strength was obtained in mortar specimens produced with 20% boron pentahydrate substitution (58.22 MPa). The lowest compressive strength was obtained in the mortar specimens containing 40% ulexite (43.32 MPa).

According to the results obtained, when the activator ratio increased from 6% Na^+ to 8% Na^+, the compressive strengths of all specimens increased at all curing times. This is found to be in accordance with the literature and it has been stated in previous studies that mechanical strengths will increase with the increase in activator ratio up to a certain level [4,5]. When the results of 3, 7, and 28 days are examined, the compressive strengths of slag binder mortars activated with colemanite, ulexite and boron pentahydrate showed similar increases.

According to the test results, it was seen that increases in compressive strengths can be obtained by substituting colemanite, ulexite, or boron pentahydrate with an alkali activator. Particularly for 10% and 20% substitution rates, it was determined that colemanite, ulexite or

boron pentahydrate provided increases in strengths at all curing times. The compressive strength increases obtained were a maximum of 40% (20 U-1) in groups containing 6% Na and a maximum of 20% (20B-2) in groups containing 8% Na^+ activator. Therefore, it is concluded that the substitution of colemanite, ulexite or boron pentahydrate with an alkaline activator behaves more efficiently in mixtures with low activator content.

In previous studies, it has been shown that colemanite and ulexite substituted with an activator in fly ash and blast furnace slag-based binder systems affect the mechanical strength results depending on alkali ratios. The results obtained in this study are consistent with the studies in the published literature [21,22,24,56].

3.3. Isothermal calorimetry measurement

In the study, reaction kinetics measurements were carried out with an isothermal calorimetry device for up to 48 hours at a 20% bor refined product replacement rate, which yielded the optimum results according to the compressive strength results. As a result of the measurements, the heat flow and total reaction heat curves of the reference pastes containing 6% Na^+ and 8% Na^+ and the slag-based pastes in which colemanite, ulexite, and boron pentahydrate were used as activator substitutes are presented in Fig. 9, Fig. 10, Fig. 11 and Fig. 12. According to Figs. 9 and 10, it was observed that a single exothermic peak emerged for the use of different sodium concentrations and boron-refined products. The presence of a single peak in the test results indicates that alkali-activated material has a different structure than that of the cement hydration product. It is known that there are two peaks in cement hydration kinetics, the first peak is related to the reaction of C_3A, and the second peak is related to the hydration products CSH gel, the result of C_2S and C_3S hydration. However, no significant second peak could be detected in the heat flow in the alkali-activated slag binder pastes. It has been observed that similar results were obtained with previously published studies regarding alkali-activated binders [57–60].

When the heat flow curves are examined for a mixture containing 6% Na^+, it is seen that the highest and sharpest peak belongs to the reference sample. Colemanite, ulexite, and boron pentahydrate replaced with activators caused the lower heat flow peaks than that of the reference sample. When the heat flow peak values obtained were examined, the highest peak value after the reference was obtained in boron pentahydrate, colemanite and ulexite, respectively. The measured heat flow peak values were determined in the range of 32–42 mW/g between 0 and 2 hours' period. When the heat flow curves of mixtures containing 8% Na^+ were examined, the highest peak values were measured in the reference mixture, similar to the mixtures containing 6% Na^+. On the other hand, the highest peak values after the reference were measured in colemanite, boron pentahydrate, and ulexite, respectively. Heat flow peak values of mixtures containing 8% Na^+ were determined to be in the range of 22–38 mW/g between 0 and 2 hours' period.

In addition, when the total heat of hydration curves (presented in Figs. 11 and 12) of mixtures for both Na^+ percentages are examined, it is seen that colemanite, ulexite and boron pentahydrate substituted

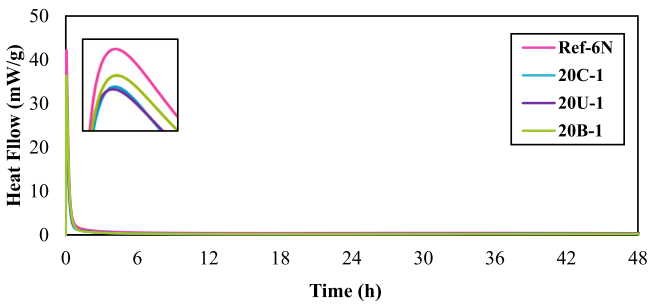

Fig. 9. The rate of hydration of first-group pastes.

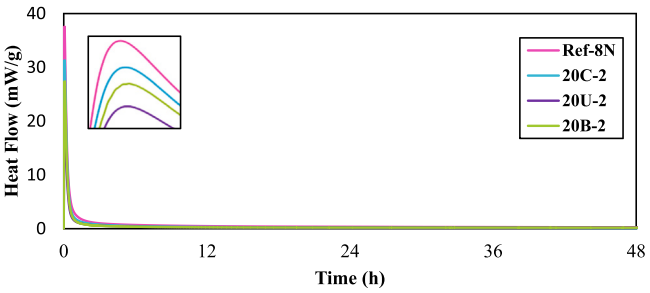

Fig. 10. The rate of hydration of second-group pastes.

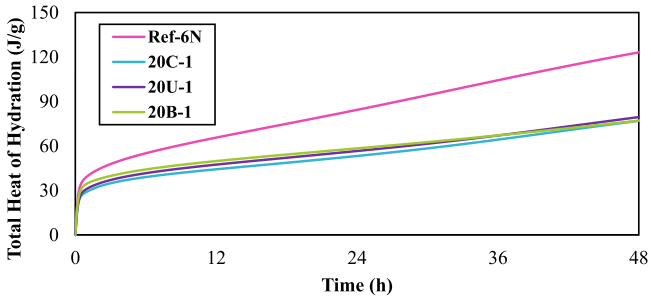

Fig. 11. The total heat of reaction of the first-group pastes.

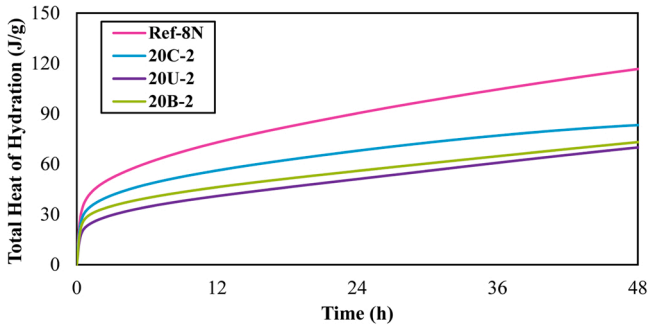

Fig. 12. The total heat of reaction of the second-group pastes.

samples gave lower total heat of hydration curves compared to the references. The obtained curves show that refined boron derivative products slow down the reaction. This situation also explains why boron substitution did not make a significant contribution to the compressive strength compared to the reference samples in the early period. When studies in the literature are examined, it is shown that refined boron products extend the setting time and are used to regulate the setting time. It has been reported in previous studies that boron products were used to bring binders, especially those with very short setting times, to a usable level by extending their setting times. In addition, this property of boron has been used to extend the setting time of alkali-activated materials subjected to room conditions or heat curing [61,62].

3.4. Thermogravimetric and Differential Thermal Analysis (TGA/DTA)

TGA and DTA analyses of reference pastes containing 6% Na^+ and 8% Na^+ and 28 days' slag binder pastes activated by replacing colemanite, ulexite and boron pentahydrate with sodium metasilicate are shown in Fig. 13 and Fig. 14. Mass losses of alkali-activated paste was occurred at different temperatures. This can be explained by different reaction products of alkali-activated paste. The mass loss that occurred up to 200°C can be explained by the evaporation of physically bound water [63–66].

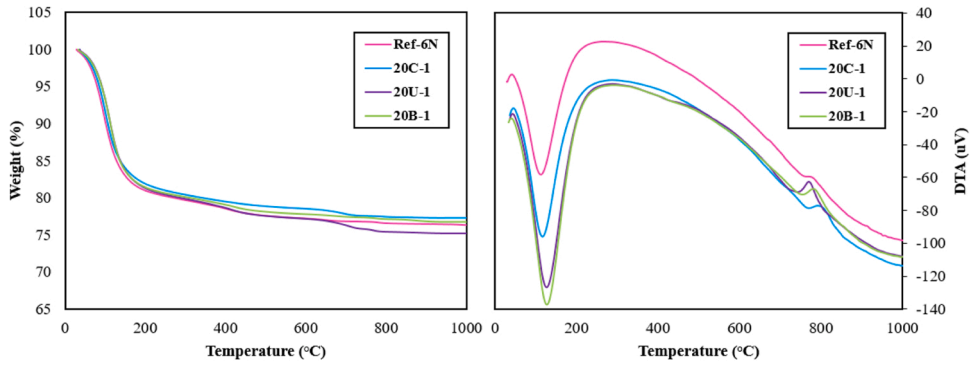

Fig. 13. Weight (%) and DTA of first-group pastes.

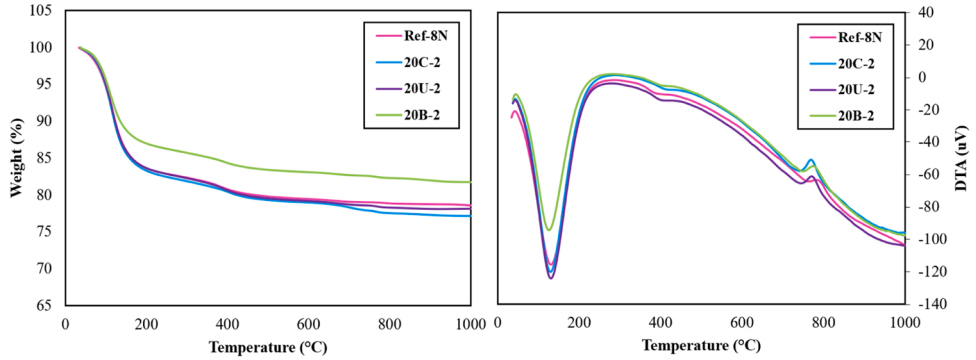

Fig. 14. Weight (%) and DTA of second-group pastes.

When Fig. 13 (mixture containing 6% Na) is examined, as a result of the evaporation of physically bound water, the weight losses of Ref-6 N, 20 C-1, 20 U-1, and 20B-1 pastes at 0–200°C are measured as 19.0%, 18.1%, 18.7% and 18.6%, respectively. Weight losses increased with the decomposition of the alkali-activated gel (C-A-S-H) between 300 and 600°C. Accordingly, the weight losses at 0–600°C were measured at 22.8%, 21.5%, 22.9% and 22.3%, respectively. Furthermore, no significant weight loss occurred between 600 and 1000°C. Total weight losses at the end of 1000°C were determined as 23.6%, 22.7%, 24.8% and 23.3%, respectively.

Similarly, as shown in Fig. 14 (mixture containing 8% Na^+) is examined, as a result of the evaporation of physically bound water, the weight losses of Ref-6 N, 20 C-1, 20 U-1, and 20B-1 pastes at 0–200°C are measured as %16.5, %16.7, %16.4 and %13.0 respectively. Weight losses increased with the decomposition of the alkali-activated gel (C-A-S-H) between 300 and 600°C. Accordingly, the weight losses at 0–600°C were found %20.6, %20.8, %21.0 and %16.8, respectively. Moreover, no significant weight loss occurred between 600 and 1000°C. Total weight losses at the end of 1000°C were determined as %21.4, %22.8, % 21.8 and %18.3, respectively.

When the weight losses in mixtures containing 6% and 8% Na^+ were compared, it was observed that lower weight loss occurred in mixtures containing 8% Na^+. This can be explained by the fact that amounts of alkaline activated bonds are intensive in mixtures containing 8% Na^+.

Replacement of colemanite and boron pentahydrate with an alkali activator in mixtures containing 6% Na^+ reduced the weight losses compared to the reference. For ulexite replacement with an alkali activator, weight loss was measured to be equivalent to the reference mixture between 0 and 600 C temperature and higher than the reference mixture between 0 and 1000°C temperature.

In mixtures containing 8% Na^+, an equivalent or higher weight loss was measured for the substitution of colemanite or ulexite in comparison to the reference mixture, while lower weight losses were measured for the substitution of boron pentahydrate compared to the reference mixture.

3.5. Inductively Coupled Plasma Mass Spectrometry (ICP-MS)

The changes in the chemical compositions of reference pastes containing 6% Na^+ and 8% Na^+ and slag binder pastes activated with colemanite, ulexite and boron pentahydrate replaced with sodium metasilicate were determined by ICP-MS analysis and the results are presented in Fig. 15. Based on the analysis results, it was determined that the highest amount of element was found to be Ca element for all specimens. In terms of amount basis, the Ca element is followed by the Na and Al elements. The highest amount of Na was measured in Ref-6 N and Ref-8 N mixtures. With the substitution of boron products, the presence of boron was observed while a decrease in the Na ratio was determined. Moreover, boron elements could not be detected in Ref-6 N and Ref-8 N samples. On the contrary, it was determined that the paste samples coded 20 C-1, 20 U-1 20B-1, 20 C-2, 20 U-2, and 20B-2, which contain boron compounds, contained 358, 410, 447, 488, 412, 428 mg/L boron element.

3.6. FESEM, EDX and elemental mapping

FESEM images of reference, colemanite, ulexite, and boron pentahydrate substituted slag-based mortars, at 28 days, containing 6% Na^+ and 8% Na^+ are shown in Fig. 16. Accordingly, gel structure, binder matrix, aggregate, micro-cracks and pores are shown in FESEM images using the literature. In FESEM images, the ITZ (interfacial transition zone), intermediate transition surface region of alkali-activated mortars, which has a high impact on mechanical strength, is shown [67–69]. The gel structure of blast furnace slag-based alkali-activated mortars shows homogeneous C-A-S-H (alumina silicate-based) and C-B-A-S-H (boron alumina silicate-based) gel structures [70].

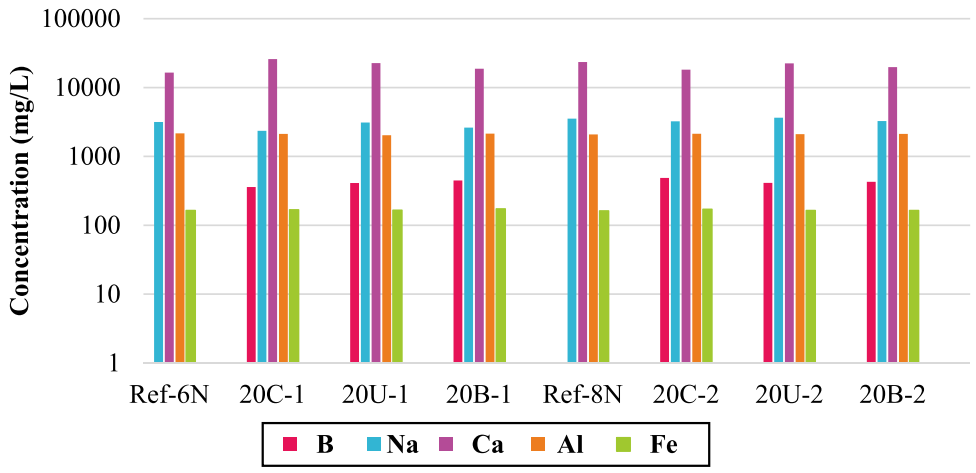

Fig. 15. Elemental concentrations of the first and second groups pastes.

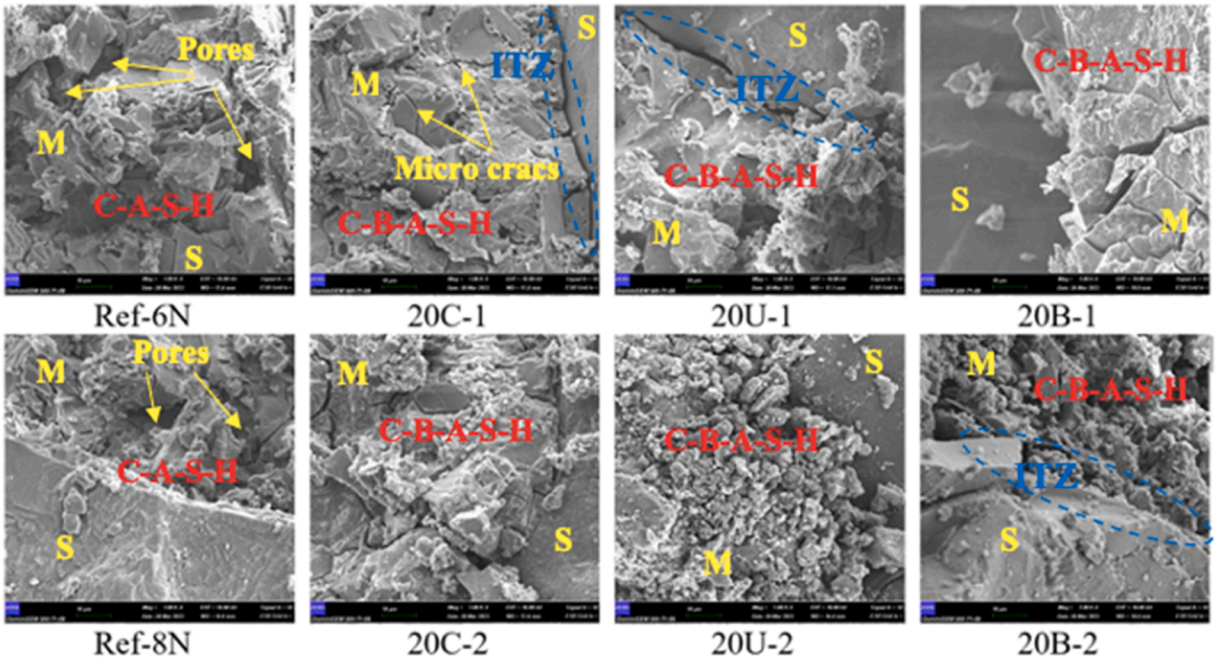

Fig. 16. FESEM images of the first and second groups mortar samples (S:Sand, M:Matrice, ITZ: Interfacial Transition Zone).

The mortars coded Ref-6 N and Ref-8 N in Fig. 16 show the microstructure of conventional alumina silicate gel. From these figures, partial cracks are observed in the structure of alumina silicate gels in the microstructure of the reference mortars. A similar crack structure was observed with colemanite replaced activator in mixtures containing both 6% Na and 8% Na. Moreover, as can be seen from the FESEM pictures, it was observed that the gel structure was more compact and had fewer microcracks in mortars made with ulexite replaced activator, unlike the microstructure of the reference mortar. Improvements in the microstructure of refined-boron products substituted as an activator at the appropriate level can be seen in some of the FESEM pictures. This result is particularly parallel to the increase in 28-day flexural and compressive strengths, thus more compact structure provides higher strength. In addition to traditional alumina silicate gels, the formation of boron-alumina-silicate gels with the addition of boron refining products as an activator replacement is thought to contribute to improvements in microstructure. Previous studies have also shown that boron-alumina-silicate gels have a positive effect on reducing the crack structure on the microstructure [21].

In addition, EDX analyzes were performed, marked in rectangles, on the gel parts of the images obtained from the reference mixture and boron-refined products and the results are shown in Fig. 17. As a result of EDX analysis, while boron components were not seen in the reference samples, the presence of boron elements was detected in the samples produced by replacing boron-refined products with the activator.

When the EDX analysis results of the samples produced with 6% Na^+ content were examined, the presence of boron element was detected in the gel structure at the rates of 13.05%, 13.74% and 9.28%, respectively, by the substitution of colemanite, ulexite and boron pentahydrate with activator. On the other hand, in the samples produced with 8% Na^+ content, the presence of boron element was detected in the gel structure at the rates of 8.54%, 10.36% and 8.49%, respectively, by the substitution of colemanite, ulexite and boron pentahydrate with activator. It is observed that the presence of boron elements in the gel structure increases as the sodium ratio in the mixture decreases. This supports the previously made conclusion that replacing colemanite, ulexite, or boron pentahydrate with an alkaline activator acts more efficiently in mixtures containing a low alkali activator.

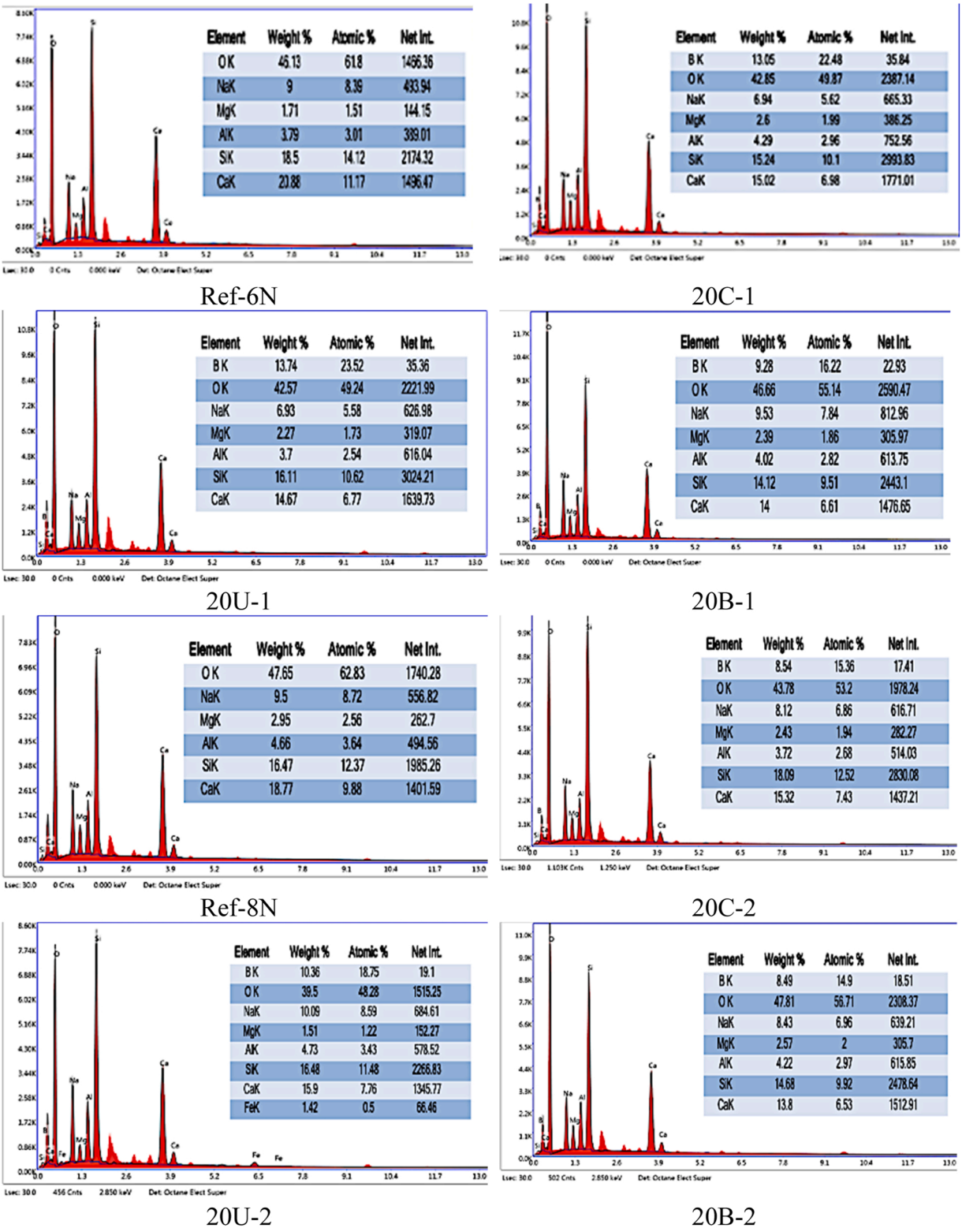

Fig. 17. EDX images of the first and second-group mortar samples.

Ratios of each element are presented in Table 6. In Figs. 18, 19, 20 and 21, mapping images of aluminosilicate gels and boroaluminosilicate gels are shown at 1000 magnification. Mapping images of reference mortar containing 6% Na^+ and 8% Na^+ and boron-refined-substituted mortars are shown in Figs. 18, 19, 20 and 21. As a result of the analysis, each element is shown with a color. Accordingly, sodium is shown in yellow, oxygen is shown in green, aluminum is shown in turquoise, silicon is shown in blue, calcium is shown in red, and boron is shown in purple color. Calcium and silicon are visualized with intense coloring in each sample. Na and Al appear to be less intensely colored than that of calcium and silicon. In reference samples (made with 6% and 8% Na^+) boron element was not seen in the microstructure; on the other hand, in mortars made with colemanite substitution, the boron element can be seen in its microstructure as a rarer purple color compared to others.

Table 6
Elements ratios.

Mixture code	Elements (%)						
	O	Na	Ca	Si	Al	B	Other
Ref-6N	24	8	14	45	7	0	2
20 C-1	18	6	18	47	7	1	3
Ref-8N	18	7	18	43	11	0	3
20 C-2	22	7	19	38	9	1	4

Moreover, there was no significant difference observed between samples made with 6% and 8% Na^+ activator ratios.

3.7. X-ray diffraction (XRD) analysis

XRD analysis results of mortar samples produced by substituting 20% colemanite, ulexite and boron pentahydrate at 6% and 8% Na^+ ratios are presented in Fig. 22 and Fig. 23. Based on the results obtained, the presence of quartz, albite, calcium silica hydrate (CSH) and calcium alumina silica hydrate (CASH) peaks were observed in the Ref-6 N and Ref-8 N samples. On the other hand, it was determined that sodium

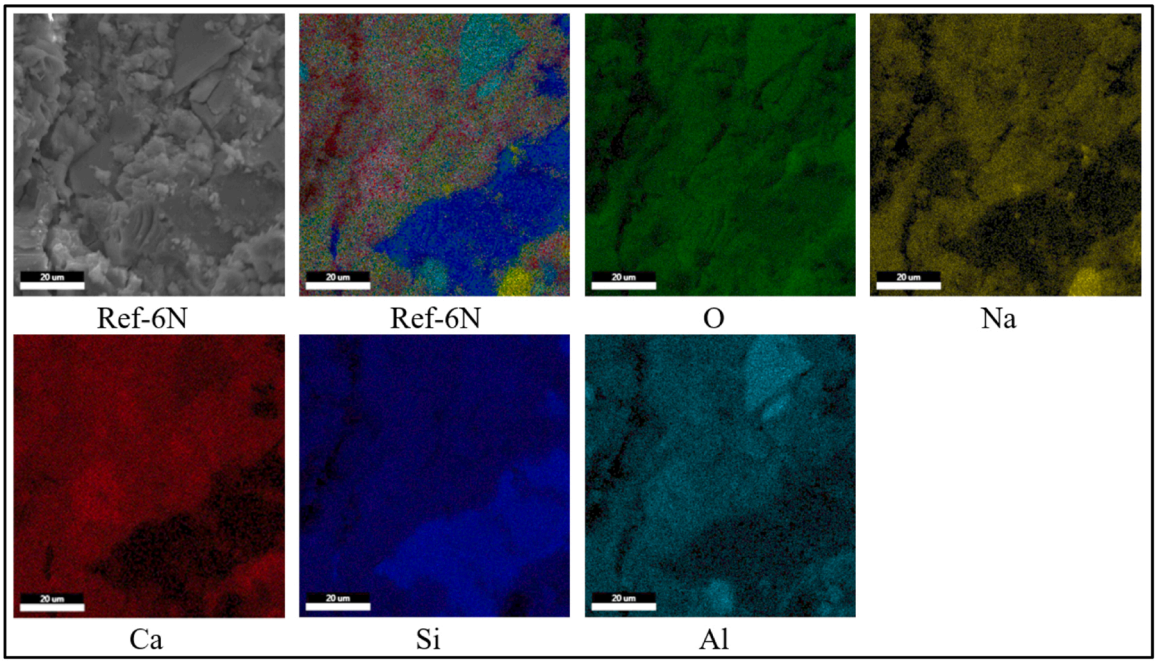

Fig. 18. Mapping image of mortar coded Ref-6 N.

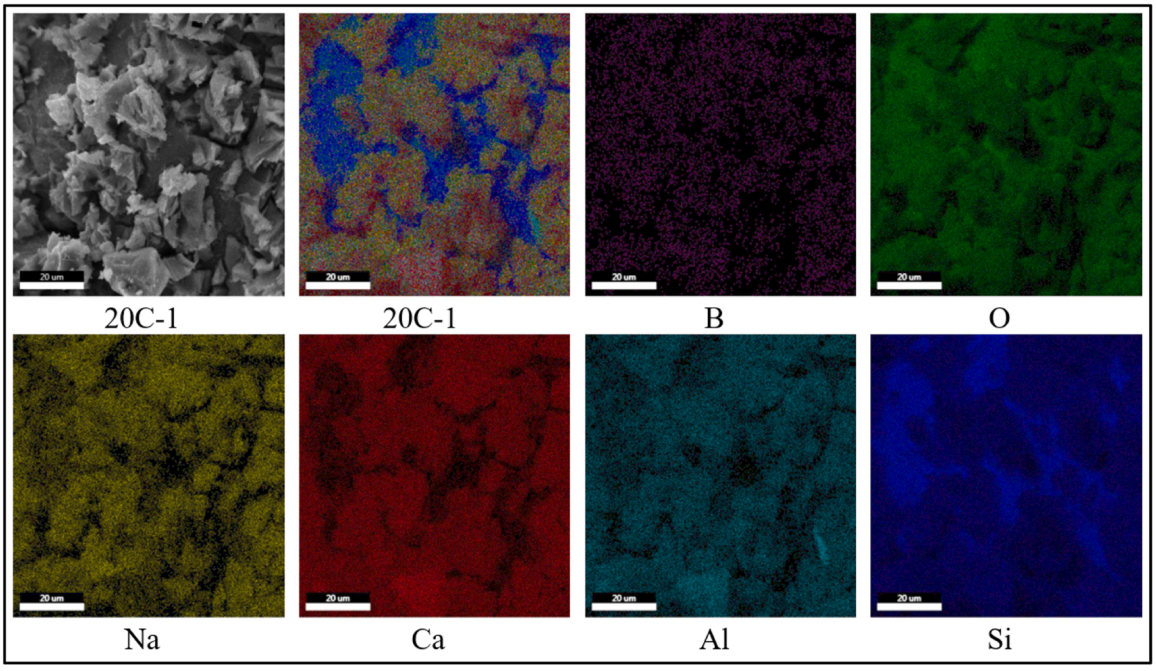

Fig. 19. Mapping image of mortar coded 20 C-1.

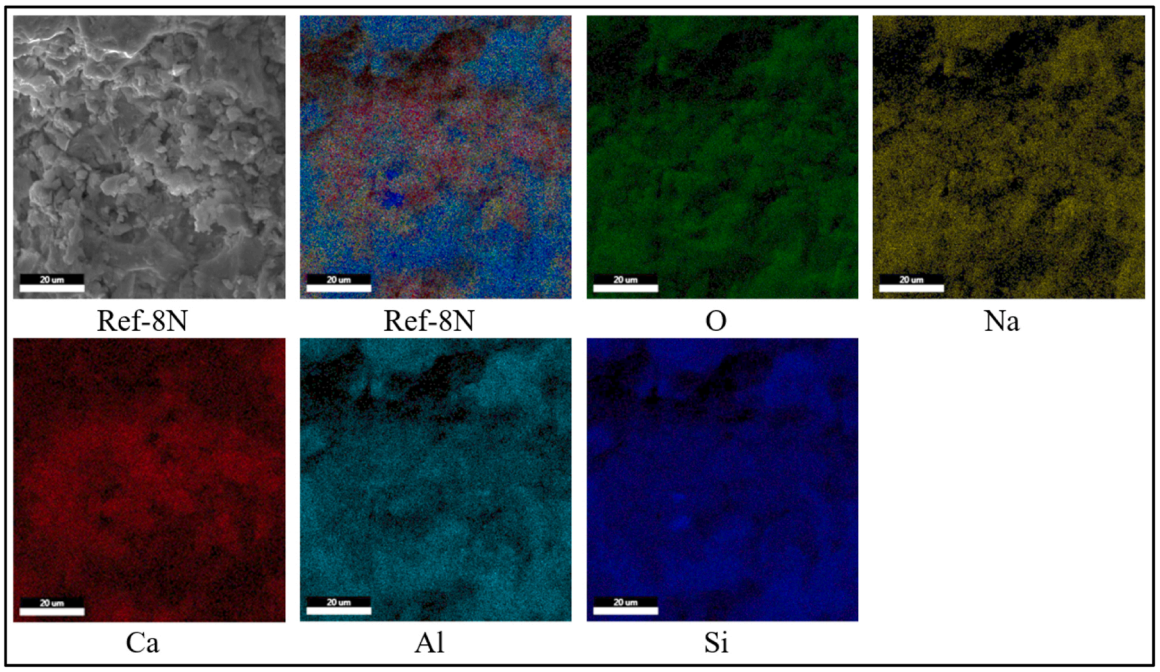

Fig. 20. Mapping image of mortar coded Ref-8 N.

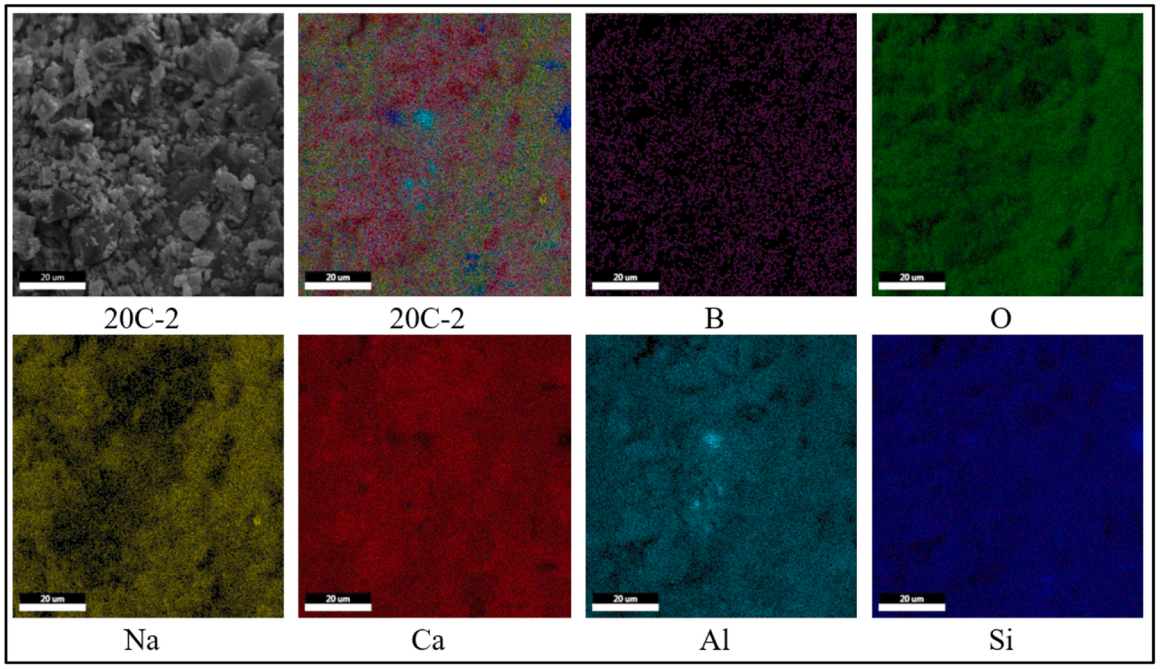

Fig. 21. Mapping image of mortar coded 20 C-2.

borate and calcium borate minerals were present in the samples with 20% colemanite, ulexite and boron pentahydrate replacement. The presence of calcium borate silica hydrate minerals was also observed in the samples produced by substituting boron-refined products. According to the XRD analysis results, the formation of minerals such as calcium borate, sodium borate and calcium borate silica hydrate (CBSH), which contain the boron element, was detected as a result of substituting boron-refined products with activators.

3.8. Life Cycle Assessment (LCA) results

This part of the study investigates the critical role of raw material transportation in determining the environmental impact of mortar formulations using two distinct transportation scenarios. In the first scenario, the actual transportation distances for each raw material were calculated, using Google Maps to gauge the exact routes from the source to the laboratory where the mortar mixtures are prepared. The comprehensive data for this scenario is highlighted and presented in Fig. 4. This methodology emphasizes the negative environmental impacts of the logistical complexities that exist in the construction sector.

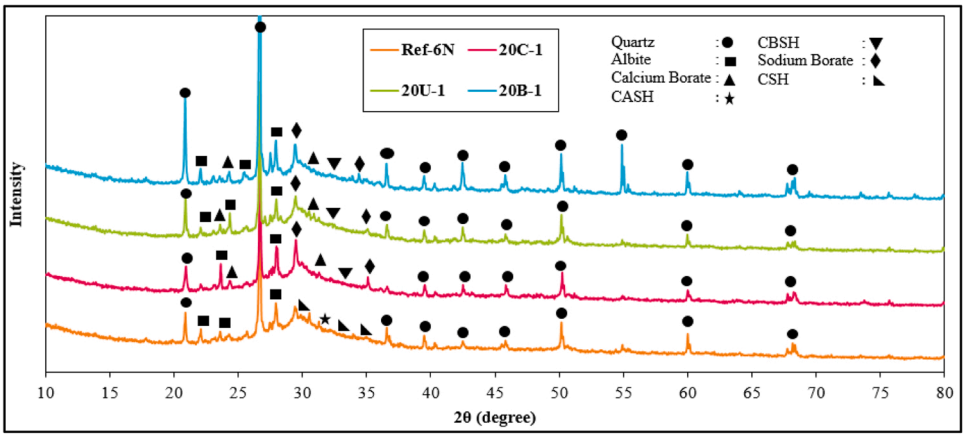

Fig. 22. XRD pattern of the first-group mortars.

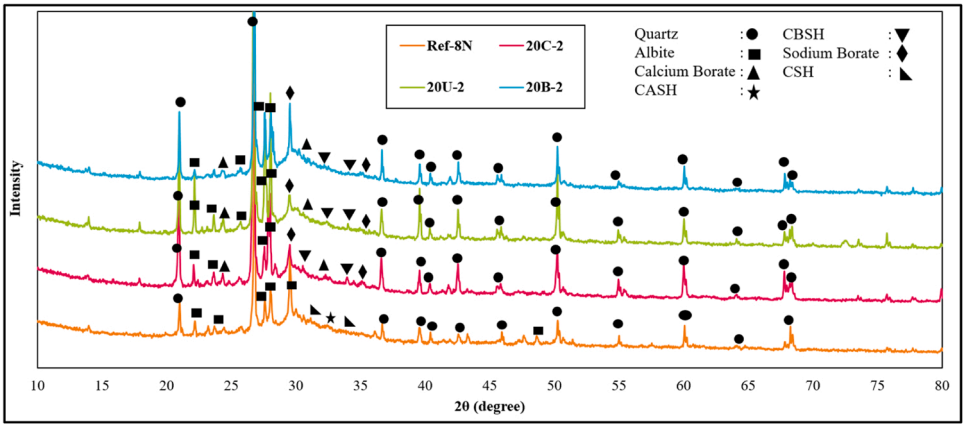

Fig. 23. XRD pattern of the second-group mortars.

In the second scenario a hypothetical approach, positing a scenario where all raw materials are sourced locally, within a uniform distance of 7 km was adopted. This simplification serves to highlight the potential environmental benefits of local sourcing, providing contrast to the initial scenario. This framework provides a means of assessing the environmental imprint resulting from decreased transportation distances. These two scenarios offer a comprehensive understanding of the transportation's impact in LCA analyses. They emphasize the importance of considering both actual logistical practices and idealized, sustainable procurement strategies in the pursuit of environmentally responsible construction methodologies.

The environmental impact category values of mortar mixtures are quantified with the CML-IA baseline method for 1 m^3 per MPa by considering the cradle-to-gate approach. This method involves 11 environmental impact categories (AD, AD-FF, GWP, ODP, HT, FAE, MAE, TE, PO, AP, and EP), and actual transportation scenario results are shown in Table 7. The value of GWP for conventional mortar with Portland cement and alkali-activated reference mortar are calculated as 1.74E+01 and 1.05E+01 kg CO_2 eq, respectively. On the other hand, GWP of the mortars with refined-boron products (colemanite, ulexite and boron pentahydrate) by 20% substitution are quantified as 8.87, 9.25, 8.85 kg CO_2 eq, respectively. According to these findings, the GWP of conventional mortars can be decreased by 39.7% through the use of mortars based on blast furnace ash and 8% Na+. Furthermore, in terms of GWP, the outcomes demonstrate that boron pentahydrate exhibits the most favorable environmental performance in comparison to the other two refined boron products (colemanite and ulexite).

The comparison of environmental impacts of mortar mixtures tested

Table 7
The environmental impact category values of mortar mixtures for 1 m^3 per Mpa with real transportation scenario (CML baseline method: V3.09/characterization).

Impact Category	Unit	PC	Ref-8N	20 C-2	20 U-2	20B-2
AD	kg Sb eq	4.86E-05	5.37E-05	4.24E-05	4.42E-05	3.95E-05
AD-FF	MJ	1.45E+02	1.32E+02	1.12E+02	1.17E+02	1.12E+02
GWP	kg CO_2 eq	1.74E+01	1.05E+01	8.87E+00	9.25E+00	8.85E+00
ODP	kg CFC-11 eq	1.19E-07	1.18E-07	1.01E-07	1.05E-07	1.49E-07
HT	kg 1,4-DB-eq	5.52E+00	6.93E+00	5.62E+00	5.87E+00	5.36E+00
FAE	kg 1,4-DB-eq	2.80E+00	3.21E+00	2.62E+00	2.73E+00	2.52E+00
MAE	kg 1,4-DB-eq	6.74E+03	6.79E+03	5.57E+03	5.82E+03	5.51E+03
TE	kg 1,4-DB-eq	4.78E-02	5.41E-02	4.33E-02	4.53E-02	4.12E-02
PO	kg C_2H_4 eq	2.29E-03	2.04E-03	1.71E-03	1.79E-03	1.69E-03
AP	kg SO_2 eq	5.09E-02	4.36E-02	3.65E-02	3.80E-02	3.59E-02
EP	kg PO4 eq	1.32E-02	1.11E-02	9.31E-03	9.71E-03	9.12E-03

Table 8
The environmental impact category values of mortar mixtures for 1 m^3 per MPa with local transportation scenario (CML baseline method: V3.09/characterization).

Impact Category	Unit	PC	Ref-8N	20 C-2	20 U-2	20B-2
AD	kg Sb eq	2.95E-05	3.09E-05	2.27E-05	2.36E-05	2.11E-05
AD-FF	MJ	6.15E+01	3.27E+01	2.67E+01	2.78E+01	3.25E+02
GWP	kg CO_2 eq	1.15E+01	3.46E+00	2.77E+00	2.90E+00	3.18E+00
ODP	kg CFC-11 eq	4.00E-08	2.41E-08	2.01E-08	2.07E-08	7.39E-08
HT	kg 1,4-DB-eq	2.63E+00	3.52E+00	2.65E+00	2.76E+00	2.61E+00
FAE	kg 1,4-DB-eq	1.56E+00	1.74E+00	1.34E+00	1.40E+00	1.33E+00
MAE	kg 1,4-DB-eq	4.25E+03	3.83E+03	3.02E+03	3.15E+03	3.14E+03
TE	kg 1,4-DB-eq	2.69E-02	2.94E-02	2.21E-02	2.30E-02	2.15E-02
PO	kg C2H4 eq	1.34E-03	9.16E-04	7.37E-04	7.70E-04	7.88E-03
AP	kg SO2 eq	3.12E-02	2.03E-02	1.63E-02	1.700E-02	1.72E-02
EP	kg PO4 eq	8.23E-03	5.21E-03	4.22E-03	4.40E-03	4.38E-03

which has optimum strengths (20% replacement with colemanite, ulexite and boron pentahydrate), reference mortar groups containing 8% Na^+ and conventional mortar mixture consisting of Portland cement with

actual transportation conditions are presented in Fig. 24. The results reveal that the mortars with boron-refined products have better environmental performance than reference mortar for almost all environmental impact categories except the ODP impact category. The mortar mixture by substituting 20% boron pentahydrate has a higher environmental impact than other mortar mixtures in terms of ODP. The main contributor component for ODP is found as steam usage in the refining process of boron pentahydrate. When conventional mortar mixture is compared with the mortars consisting of boron-refined products, the mortars with boron-refined products have 47–49% lower environmental impacts in terms of GWP which is a significant indicator of the environmental performance of a product or system. In contrast, for the impact categories of AD, HT, FAE, and TE, reference mortar exhibits the worst environmental performance in comparison to conventional mortar and mortars containing boron-refined products. The main reason for this use of sodium metasilicate and its transportation (3500 km).

Within the scope of this study, the environmental impacts of transporting raw materials for all mortar mixtures are assessed by applying a local transportation scenario. This approach provides a comprehensive understanding of the environmental aspects of mortar production, with a specific focus on the role of local transportation in the overall sustainability of construction materials. In this scenario, it is assumed that all raw materials are transported from a distance of 7 km, indicating that all raw materials are sourced from local sources. Fig. 25 shows the comparison of the environmental impacts of mortar mixtures with optimum strengths (20% replacement with colemanite, ulexite, and boron pentahydrate), reference mortar groups containing 8% Na+, and a conventional mortar mixture with a local transportation scenario. The findings indicate that the utilization of locally available raw materials considerably decreases the overall environmental impacts of mortar mixtures (Figs. 24 and 25). In the actual transportation scenario, the environmental impact difference between conventional mortar mixture and mortars containing boron-refined products (20 U-2, 20 C-2 and 20B-2) ranged from 47% to 49% (Fig. 24). However, in the local transportation scenario, this difference increased from 72% to 75% in terms of GWP (Fig. 25).

The local transportation scenario results of mortar mixtures are given in Fig. 25. Similar to the first scenario, LCA analyses were performed to quantify the environmental impacts of mortar mixtures for 1 m^3 per MPa using the CML-IA baseline method. The value of GWP for conventional mortar with Portland cement and reference mortar were calculated as 1.15E+01 and 3.46 kg CO_2 eq, respectively. On the other hand, the GWP of the mortars with refined boron products (colemanite, ulexite and boron pentahydrate) by 20% substitution was quantified as 2.77, 2.90, 3.18 kg CO_2 eq, respectively. With the local transportation scenario, the GWP of conventional mortar reduced by 34% (from 1.74E+01–1.15E+01 kg CO_2 eq), while the reference mortar had a decrease of 67% % (from 1.05E+01–3.46 kg CO_2 eq). Furthermore, the GWP of mortars containing refined boron products (20 C-2, 20 U-2 and 20B-2) has been decreased by 64–69% which is a significant reduction as a result of the local transportation scenario. The literature also has shown that the transportation of raw materials has a significant impact on the environmental performance of cementitious materials, mortars, and concrete. For instance, Patrisia et. al (2022) performed an LCA on alkali-activated concretes to assess their environmental performance by using the CML-IA Baseline method. They also found that transportation

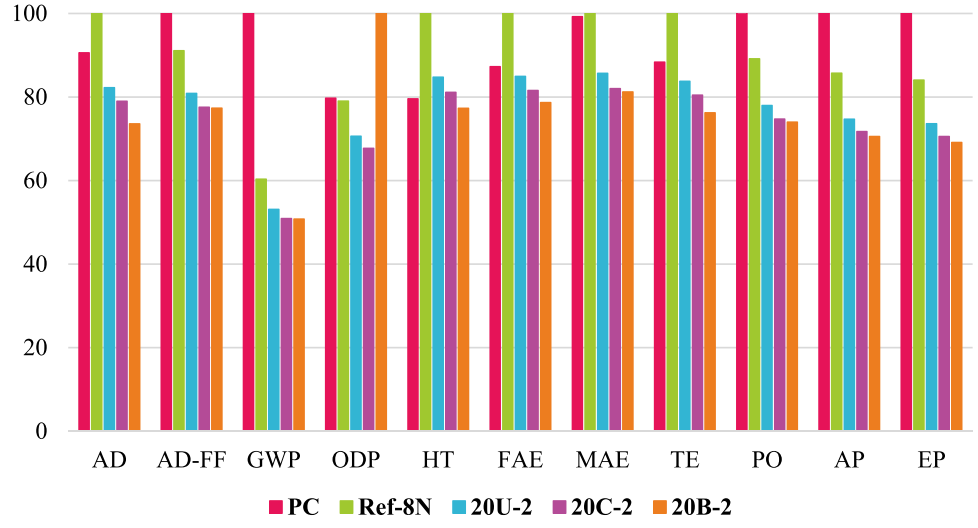

Fig. 24. The comparison of environmental impacts of mortar mixtures with real transportation scenario.

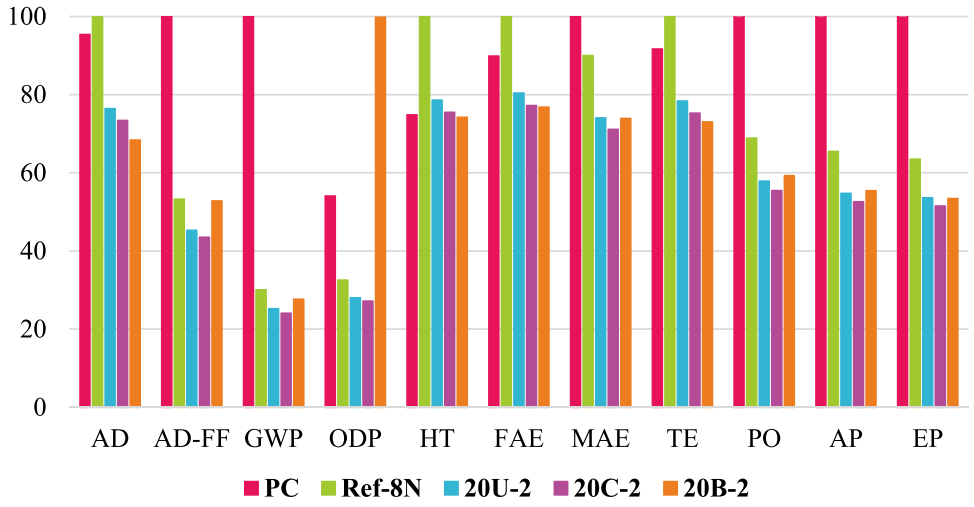

Fig. 25. The comparison of environmental impacts of mortar mixtures with local transportation scenario.

of raw materials has a significant share of around 40% of total environmental impact [71]. Besides, Nguyen et. al (2018) emphasized transportation as a key aspect in the environmental assessment of several types of finished cementitious products, such as ordinary portland cement (OPC), blended OPC with slag, blended OPC with fly ash, metakaolin-based geopolymer, and high-volume limestone alkali-activated slag cement. According to their analysis, the environmental impacts of the supply chain are greatly influenced by the location of the raw material source and the mode of transportation, accounting for up to 80% of greenhouse gas emissions [72].

The distribution of environmental impacts by production steps and sub-components for reference mortar and mortars containing refined boron products (colemanite, ulexite, and boron pentahydrate) is indicated in Fig. 26. Fig. 26 (a) illustrates that sodium metasilicate is the primary contributing component in the reference mortar for all environmental impacts, with a range of 45.5–89.7%. In particular, sodium metasilicate accounts for 52.8% of the overall GWP of the reference mortar. Similarly, Ramagiri and Kar (2021) found that sodium silicate accounts for around 50–59% of GWP in alkali-activated mortar in their study to conduct a LCA of alkali-activated mortar manufactured using precursors and activators derived from industrial waste [73]. Following sodium metasilicate, silica sand constitutes as second main component, accounting for 9–43% of the total environmental impacts of Ref-8 N.

As shown in Fig. 26 (b), sodium metasilicate is the main component responsible for the environmental impact in mortars containing colemanite (20 C-2), ranging from 39.1% to 87.4%. Similarly, in mortars containing ulexite (20 U-2), sodium metasilicate accounts for 39.4–87.4% of the total environmental impacts (Fig. 26 (c). The distribution of environmental impacts by production steps and sub-components for mortar containing boron pentahydrate (20B-2) is indicated in Fig. 26 (d). Sodium metasilicate is identified as the main material responsible for all environmental impacts of 20B-2, accounting for a percentage range of 9.9–86.8%, except for ODP. The main impacts of ODP arise from the refining process of boron pentahydrate, specifically the utilization of steams in the refining process. Moreover, boron pentahydrate (1–75.3%) and silica sand (10.9–41.5%) are the other most significant contributors to the total environmental impacts of mortar containing boron pentahydrate Fig. 26 (d).

4. Conclusion

1-Replacement colemanite, ulexite or boron pentahydrate with an alkali activator results in an increase in compressive and flexural strengths at a 20% replacement ratio. Moreover, replacing a boron-refined product with an alkali activator was more effective at low activator content.

2- Colemanite, ulexite, and boron pentahydrate replacement with an activator caused lower heat flow peaks and the total heat of hydration curves than that of the reference sample. Also, TGA analysis show that replacement of colemanite and boron pentahydrate with alkali activator in mixtures containing 6% Na^+ reduced the weight losses compared to the reference. For ulexite replacement with alkali activator, weight loss was measured to be equivalent or higher to the reference mixture. In mixtures containing 8% Na^+, an equivalent or higher weight loss was measured for the substitution of colemanite or ulexite in comparison to the reference mixture, while lower weight losses were measured for the substitution of boron pentahydrate compared to the reference mixture.

3-ICP-MS analysis results showed that while boron element could not be detected in Ref-6 N and Ref-8 N samples, it was determined that the paste samples coded 20 C-1, 20 U-1 20B-1, 20 C-2, 20 U-2 and 20B-2, which contain boron compounds, contained 358, 410, 447, 488, 412, 428 mg/L boron element. Moreover, FESEM, EDX and elemental mapping show that boron refined products usage result with more compact and had fewer micro cracks microstructure in comparison to reference sample. Furthermore, as the sodium ratio in the mixture decrease from 8% to 6%, the presence of boron element in the gel structure increases.

4-XRD analysis results indicated that the formation of minerals such as calcium borate, sodium borate and calcium borate silica hydrate, which contain the boron element, was detected as a result of substituting boron refined products with activators. This showed that boron refined product participated in reaction.

5-Based on LCA analysis, the mortars consist of boron refined products have better environmental performance than reference mortar for almost all environmental impact categories. In addition, LCA results showed that transportation has a very crucial role in the environmental effects indicating the importance of supplying raw materials from local sources.

CRediT authorship contribution statement

Sedat Gulcimen: Writing – original draft, Software. **Nigmet Uzal:** Writing – review & editing, Data curation. **Ugur Durak:** Writing – original draft, Visualization. **Cengiz Duran Atis:** Writing – review & editing, Supervision. **Burak Uzal:** Validation, Methodology. **Okan Karahan:** Supervision, Conceptualization. **Ezgi Örklemez:** Writing – original draft, Investigation, Funding acquisition. **Serhan Ilkentapar:** Investigation, Funding acquisition.

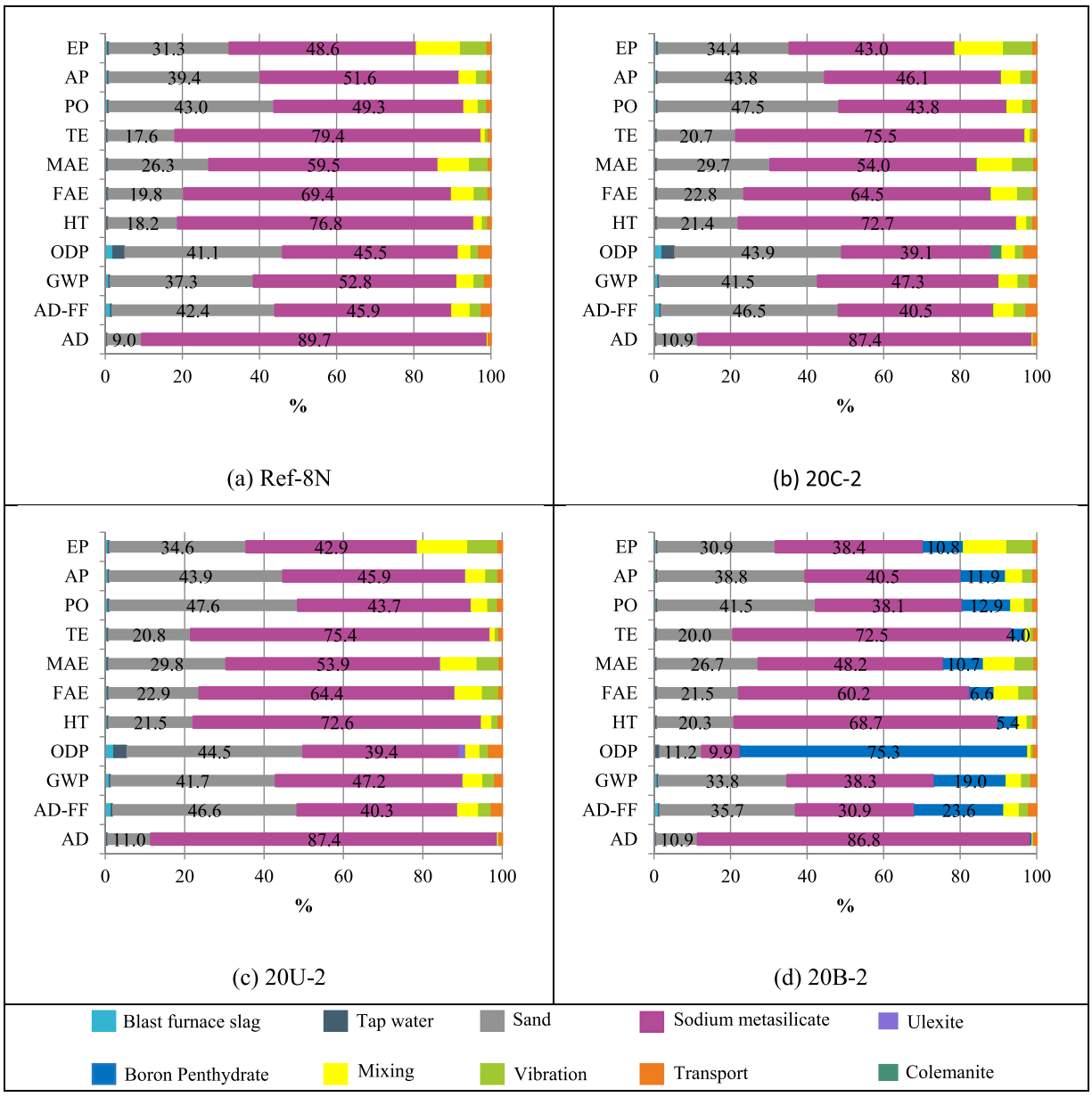

Fig. 26. The distribution of environmental impacts of mortar mixtures by sub-components with local transportation scenario.

Declaration of Competing Interest

The authors declare the following financial interests/personal relationships which may be considered as potential competing interests: Serhan Ilkentapar reports financial support was provided by Erciyes University. Ezgi Orklemez reports a relationship with Council of Higher Education of the Republic of Turkey that includes: funding grants. If there are other authors, they declare that they have no known competing financial interests or personal relationships that could have appeared to influence the work reported in this paper.

Data availability

Data will be made available on request.

Acknowledgment

This study is supported by YOK 100/2000 scholarship. This work with project code FDK-2022–12186 is supported by Erciyes University Scientific Research Project Coordination Unit.

Appendix A. Supporting information

Supplementary data associated with this article can be found in the online version at doi:10.1016/j.conbuildmat.2024.136078.

References

[1] D. Koumpouri, G.N. Angelopoulos, Effect of boron waste and boric acid addition on the production of low energy belite cement, Cem. Concr. Compos vol. 68 (2016) 1–8, https://doi.org/10.1016/J.CEMCONCOMP.2015.12.009.
[2] I.B. Topçu and A.R. Boğa, "Effect of boron waste on the properties of mortar and concrete," https://doi.org/10.1177/0734242×09345561, vol. 28, no. 7, pp. 626–633, 2009, doi: 10.1177/0734242×09345561.
[3] H.E. Galal Mors, Diatomite: its characterization, modifications and applications, Asian J. Mater. Sci. vol. 2 (3) (2010) 121–136, https://doi.org/10.3923/AJMSKR.2010.121.136.
[4] A. Özsoy, E. Örklemez, S. İlkentapar, Effect of addition diatomite powder on mechanical strength, elevated temperature resistance and microstructural properties of industrial waste fly ash-based geopolymer, J. Mater. Cycles Waste

Manag vol. 25 (4) (2023) 2338–2349, https://doi.org/10.1007/S10163-023-01692-X/METRICS.
[5] Bingöl, et al., An investigation of resistance of sodium meta silicate activated slag mortar to acidic and basic mediums, Rev. De. la construcciÓN. vol. 19 (1) (2020) 127–133, https://doi.org/10.7764/RDLC.19.1.127-133.
[6] H. Karakaş, et al., Properties of fly ash-based lightweight-geopolymer mortars containing perlite aggregates: Mechanical, microstructure, and thermal conductivity coefficient, Constr. Build. Mater. vol. 362 (2023) 129717, https://doi.org/10.1016/J.CONBUILDMAT.2022.129717.
[7] C. Shi, A.F. Jiménez, A. Palomo, New cements for the 21st century: The pursuit of an alternative to Portland cement, Cem. Concr. Res vol. 41 (7) (2011) 750–763, https://doi.org/10.1016/J.CEMCONRES.2011.03.016.
[8] J.S.J. Van Deventer, J.L. Provis, P. Duxson, Technical and commercial progress in the adoption of geopolymer cement, Min. Eng. vol. 29 (2012) 89–104, https://doi.org/10.1016/J.MINENG.2011.09.009.
[9] J.L. Provis and S.A. Bernal, "Geopolymers and Related Alkali-Activated Materials," https://doi.org/10.1146/annurev-matsci-070813-113515, vol. 44, pp. 299–327, 2014, doi: 10.1146/ANNUREV-MATSCI-070813-113515.
[10] A.F. Abdalqader, F. Jin, A. Al-Tabbaa, Development of greener alkali-activated cement: utilisation of sodium carbonate for activating slag and fly ash mixtures, J. Clean. Prod. vol. 113 (2016) 66–75, https://doi.org/10.1016/J.JCLEPRO.2015.12.010.
[11] F. Puertas, et al., Alkali-activated slag concrete: Fresh and hardened behaviour, Cem. Concr. Compos vol. 85 (2018) 22–31, https://doi.org/10.1016/J.CEMCONCOMP.2017.10.003.
[12] H.Y. Zhang, J.C. Liu, B. Wu, Mechanical properties and reaction mechanism of one-part geopolymer mortars, Constr. Build. Mater. vol. 273 (2021) 121973, https://doi.org/10.1016/J.CONBUILDMAT.2020.121973.
[13] E. Dişçi, R. Polat, The influence of nano-CaO and nano-Al2O3 and curing conditions on perlite based geopolymer concrete produced by the one-part mixing method, Constr. Build. Mater. vol. 346 (2022) 128484, https://doi.org/10.1016/J.CONBUILDMAT.2022.128484.
[14] T. Luukkonen, Z. Abdollahnejad, J. Yliniemi, P. Kinnunen, M. Illikainen, One-part alkali-activated materials: A review, Cem. Concr. Res vol. 103 (2018) 21–34, https://doi.org/10.1016/J.CEMCONRES.2017.10.001.
[15] B. Nematollahi, J. Sanjayan, F.U.A. Shaikh, Synthesis of heat and ambient cured one-part geopolymer mixes with different grades of sodium silicate, Ceram. Int vol. 41 (4) (2015) 5696–5704, https://doi.org/10.1016/J.CERAMINT.2014.12.154.
[16] M. Almakhadmeh, A.M. Soliman, Effects of mixing water temperatures on properties of one-part alkali-activated slag paste, Constr. Build. Mater. vol. 266 (2021) 121030, https://doi.org/10.1016/J.CONBUILDMAT.2020.121030.
[17] I.P. Segura, et al., "Comparison of One-Part and Two-Part Alkali-Activated Metakaolin and Blast Furnace Slag, J. Sustain. Metall. vol. 8 (4) (2022) 1816–1830, https://doi.org/10.1007/S40831-022-00606-9/FIGURES/11.
[18] R.P. Williams, A. van Riessen, Development of alkali activated borosilicate inorganic polymers (AABSIP), J. Eur. Ceram. Soc. vol. 31 (8) (2011) 1513–1516, https://doi.org/10.1016/J.JEURCERAMSOC.2011.02.021.
[19] L.P. Liu, X.M. Cui, Y. He, S.D. Liu, S.Y. Gong, The phase evolution of phosphoric acid-based geopolymers at elevated temperatures, Mater. Lett. vol. 66 (1) (2012) 10–12, https://doi.org/10.1016/J.MATLET.2011.08.043.
[20] A.T. Durant, K.J.D. MacKenzie, Synthesis of sodium and potassium aluminogermanate inorganic polymers, Mater. Lett. vol. 65 (13) (2011) 2086–2088, https://doi.org/10.1016/J.MATLET.2011.04.008.
[21] A. Nazari, A. Maghsoudpour, J.G. Sanjayan, Characteristics of boroaluminosilicate geopolymers, Constr. Build. Mater. vol. 70 (2014) 262–268, https://doi.org/10.1016/J.CONBUILDMAT.2014.07.087.
[22] A. Bagheri, A. Nazari, J.G. Sanjayan, P. Rajeev, Alkali activated materials vs geopolymers: Role of boron as an eco-friendly replacement, Constr. Build. Mater. vol. 146 (2017) 297–302, https://doi.org/10.1016/J.CONBUILDMAT.2017.04.137.
[23] A. Bagheri, A. Nazari, J.G. Sanjayan, P. Rajeev, W. Duan, Fly ash-based boroaluminosilicate geopolymers: Experimental and molecular simulations, Ceram. Int vol. 43 (5) (2017) 4119–4126, https://doi.org/10.1016/J.CERAMINT.2016.12.020.
[24] A. Bagheri, et al., Microstructural study of environmentally friendly boroaluminosilicate geopolymers, J. Clean. Prod. vol. 189 (2018) 805–812, https://doi.org/10.1016/J.JCLEPRO.2018.04.034.
[25] T. Revathi, R. Jeyalakshmi, Fly ash–GGBS geopolymer in boron environment: A study on rheology and microstructure by ATR FT-IR and MAS NMR, Constr. Build. Mater. vol. 267 (2021) 120965, https://doi.org/10.1016/j.conbuildmat.2020.120965.
[26] Y.C. Ersan, S. Gulcimen, T.N. Imis, O. Saygin, N. Uzal, Life cycle assessment of lightweight concrete containing recycled plastics and fly ash, Eur. J. Environ. Civ. Eng. vol. 26 (7) (2022) 2722–2735, https://doi.org/10.1080/19648189.2020.1767216.
[27] A. Josa, A. Aguado, A. Cardim, E. Byars, Comparative analysis of the life cycle impact assessment of available cement inventories in the EU, Cem. Concr. Res vol. 37 (5) (2007) 781–788, https://doi.org/10.1016/J.CEMCONRES.2007.02.004.
[28] "ISO 14040:2006 - Environmental management — Life cycle assessment — Principles and framework." Accessed: Nov. 13, 2023. [Online]. Available: https://www.iso.org/standard/37456.html.
[29] P.S. Matheu, K. Ellis, B. Varela, Comparing the Environmental Impacts of Alkali Activated Mortar and Traditional Portland Cement Mortar using Life Cycle Assessment, IOP Conf. Ser. Mater. Sci. Eng. vol. 96 (1) (2015) 012080, https://doi.org/10.1088/1757-899X/96/1/012080.
[30] L. Nguyen, A.J. Moseson, Y. Farnam, S. Spatari, Effects of composition and transportation logistics on environmental, energy and cost metrics for the production of alternative cementitious binders, J. Clean. Prod. vol. 185 (2018) 628–645, https://doi.org/10.1016/J.JCLEPRO.2018.02.247.
[31] R. Robayo-Salazar, J. Mejía-Arcila, R. Mejía de Gutiérrez, E. Martínez, Life cycle assessment (LCA) of an alkali-activated binary concrete based on natural volcanic pozzolan: A comparative analysis to OPC concrete, Constr. Build. Mater. vol. 176 (2018) 103–111, https://doi.org/10.1016/J.CONBUILDMAT.2018.05.017.
[32] A. Passuello, et al., Evaluation of the potential improvement in the environmental footprint of geopolymers using waste-derived activators, J. Clean. Prod. vol. 166 (2017) 680–689, https://doi.org/10.1016/J.JCLEPRO.2017.08.007.
[33] J.C.B. Moraes, et al., Durability to chemical attacks and life cycle assessment of alkali-activated binders based on blast furnace slag and sugar cane straw ash, J. Build. Eng. vol. 76 (2023) 107261, https://doi.org/10.1016/J.JOBE.2023.107261.
[34] D.A. Salas, A.D. Ramirez, N. Ulloa, H. Baykara, A.J. Boero, Life cycle assessment of geopolymer concrete, Constr. Build. Mater. vol. 190 (2018) 170–177, https://doi.org/10.1016/J.CONBUILDMAT.2018.09.123.
[35] R. Bajpai, K. Choudhary, A. Srivastava, K.S. Sangwan, M. Singh, Environmental impact assessment of fly ash and silica fume based geopolymer concrete, J. Clean. Prod. vol. 254 (2020) 120147, https://doi.org/10.1016/J.JCLEPRO.2020.120147.
[36] B. Gopalakrishna and P. Dinakar, "Life cycle assessment (LCA) and the influence of alkaline activator content on mechanical and microstructural properties of geopolymer mortar," 2024, doi: 10.1016/j.jer.2024.01.010.
[37] R. Bajpai, K. Choudhary, A. Srivastava, K.S. Sangwan, M. Singh, Environmental impact assessment of fly ash and silica fume based geopolymer concrete, J. Clean. Prod. vol. 254 (2020) 120147, https://doi.org/10.1016/J.JCLEPRO.2020.120147.
[38] S. Pradhan, Z. Li, S. Qian, A thermo-mechano-chemical activation technique to use quartz rich marine clay for one-part geopolymer preparation, Cem. Concr. Compos vol. 140 (2023) 105057, https://doi.org/10.1016/J.CEMCONCOMP.2023.105057.
[39] A.Z. Khalifa, et al., Advances in alkali-activation of clay minerals, Cem. Concr. Res vol. 132 (2020) 106050, https://doi.org/10.1016/J.CEMCONRES.2020.106050.
[40] TS EN 196-1, Methods of testing cement—part:1 determination of strength. Ankara, Turkey: TSE, 2016..
[41] C. Bilim, O. Karahan, C.D. Atiş, S. İlkentapar, Influence of admixtures on the properties of alkali-activated slag mortars subjected to different curing conditions, Mater. Des. vol. 44 (2013) 540–547, https://doi.org/10.1016/j.matdes.2012.08.049.
[42] Ş. Bingöl, C. Bilim, C.D. Atiş, U. Durak, "Durability Properties of Geopolymer Mortars Containing Slag,", Iran. J. Sci. Technol., Trans. Civ. Eng. vol. 44 (S1) (2020) https://doi.org/10.1007/s40996-019-00337-0.
[43] O. Karahan, Z. Almaz, İ.İ. Atabey, "Investigation of Physıcal and Mechanical Properties of Waste EPS Aggregate Lightweigth Concrete.", Sci. Res. Proj. Coord. Unit. Erciyes Univ., Kayseri (2016) 1–42.
[44] R.B. Meshram, S. Kumar, Comparative life cycle assessment (LCA) of geopolymer cement manufacturing with Portland cement in Indian context, Int. J. Environ. Sci. Technol. vol. 19 (6) (2022) 4791–4802, https://doi.org/10.1007/s13762-021-03336-9.
[45] Y. Patrisia, D.W. Law, C. Gunasekara, A. Wardhono, Life cycle assessment of alkali-activated concretes under marine exposure in an Australian context, Environ. Impact Assess. Rev. vol. 96 (2022) 106813, https://doi.org/10.1016/j.eiar.2022.106813.
[46] A. Alsalman, L.N. Assi, R.S. Kareem, K. Carter, P. Ziehl, Energy and CO2 emission assessments of alkali-activated concrete and Ordinary Portland Cement concrete: A comparative analysis of different grades of concrete, Clean. Environ. Syst. vol. 3 (2021) 100047, https://doi.org/10.1016/j.cesys.2021.100047.
[47] S. Fernando, C. Gunasekara, D.W. Law, M.C.M. Nasvi, S. Setunge, R. Dissanayake, Life cycle assessment and cost analysis of fly ash–rice husk ash blended alkali-activated concrete, J. Environ. Manag. vol. 295 (2021) 113140, https://doi.org/10.1016/j.jenvman.2021.113140.
[48] K.K. Ramagiri, A. Kar, Environmental impact assessment of alkali-activated mortar with waste precursors and activators, J. Build. Eng. vol. 44 (2021) 103391, https://doi.org/10.1016/j.jobe.2021.103391.
[49] S.R. Prusty, R. Panigrahi, S. Jena, Characterisation and life-cycle assessment of alkali-activated concrete using industrial wastes, Int. J. Environ. Sci. Technol. (2023), https://doi.org/10.1007/s13762-023-05100-7.
[50] B. Kanagaraj, N. Anand, U. Johnson Alengaram, R. Samuvel Raj, Engineering properties, sustainability performance and life cycle assessment of high strength self-compacting geopolymer concrete composites, Constr. Build. Mater. vol. 388 (2023) 131613, https://doi.org/10.1016/j.conbuildmat.2023.131613.
[51] TSE, Ankara, Turkey, 2020.
[52] T. Standard, "Turkish Standard Ts 2824 En 1338," no. 112, 2005..
[53] "ISO 14044:2006 - Environmental management — Life cycle assessment — Requirements and guidelines." Accessed: Nov. 14, 2023. [Online]. Available: https://www.iso.org/standard/38498.html.
[54] T. Türkbay, B. Laratte, A. Çolak, S. Çoruh, B. Elevli, Life Cycle Assessment of Boron Industry from Mining to Refined Products, Sustain. (Switz.) vol. 14 (3) (Feb. 2022) 1787, https://doi.org/10.3390/SU14031787/S1.
[55] "SimaPro Expert.".
[56] P. Rożek, P. Florek, M. Król, W. Mozgawa, Immobilization of Heavy Metals in Boroaluminosilicate Geopolymers, Materials vol. 14 (1) (2021) 214, https://doi.org/10.3390/MA14010214.
[57] Z. Sun, A. Vollpracht, Isothermal calorimetry and in-situ XRD study of the NaOH activated fly ash, metakaolin and slag, Cem. Concr. Res vol. 103 (2018) 110–122, https://doi.org/10.1016/J.CEMCONRES.2017.10.004.

[58] X. Yao, Z. Zhang, H. Zhu, Y. Chen, Geopolymerization process of alkali–metakaolinite characterized by isothermal calorimetry, Thermochim. Acta vol. 493 (1–2) (2009) 49–54, https://doi.org/10.1016/J.TCA.2009.04.002.
[59] S.K. Nath, S. Kumar, Influence of iron making slags on strength and microstructure of fly ash geopolymer, Constr. Build. Mater. vol. 38 (2013) 924–930, https://doi.org/10.1016/J.CONBUILDMAT.2012.09.070.
[60] A.H. Mahmood, M. Babaee, S.J. Foster, A. Castel, Capturing the early-age physicochemical transformations of alkali-activated fly ash and slag using ultrasonic pulse velocity technique, Cem. Concr. Compos vol. 130 (2022) 104529, https://doi.org/10.1016/J.CEMCONCOMP.2022.104529.
[61] F. Souayfan, E. Rozière, A. Loukili, C. Justino, Effect of Retarders on the Reactivity and Hardening Rate of Alkali-Activated Blast Furnace Slag Grouts, Mater. (Basel) vol. 16 (17) (2023) 5824, https://doi.org/10.3390/MA16175824.
[62] C. Dupuy, et al., Formulation of an alkali-activated grout based on Callovo-Oxfordian argillite for an application in geological radioactive waste disposal, Constr. Build. Mater. vol. 232 (2020) 117170, https://doi.org/10.1016/J.CONBUILDMAT.2019.117170.
[63] A. Rafeet, R. Vinai, M. Soutsos, W. Sha, Effects of slag substitution on physical and mechanical properties of fly ash-based alkali activated binders (AABs), Cem. Concr. Res vol. 122 (2019) 118–135, https://doi.org/10.1016/J.CEMCONRES.2019.05.003.
[64] I. Hager, M. Sitarz, K. Mróz, Fly-ash based geopolymer mortar for high-temperature application – Effect of slag addition, J. Clean. Prod. vol. 316 (2021) 128168, https://doi.org/10.1016/J.JCLEPRO.2021.128168.
[65] J.C. Kuri, S. Majhi, P.K. Sarker, A. Mukherjee, Microstructural and non-destructive investigation of the effect of high temperature exposure on ground ferronickel slag blended fly ash geopolymer mortars, J. Build. Eng. vol. 43 (2021) 103099, https://doi.org/10.1016/J.JOBE.2021.103099.
[66] M. Riaz Ahmad, M. Khan, A. Wang, Z. Zhang, J.G. Dai, Alkali-activated materials partially activated using flue gas residues: An insight into reaction products, Constr. Build. Mater. vol. 371 (2023) 130760, https://doi.org/10.1016/J.CONBUILDMAT.2023.130760.
[67] E. Pawluczuk, K. Kalinowska-Wichrowska, J.R. Jiménez, J.M. Fernández-Rodríguez, D. Suescum-Morales, Geopolymer concrete with treated recycled aggregates: Macro and microstructural behavior, J. Build. Eng. vol. 44 (2021) 103317, https://doi.org/10.1016/J.JOBE.2021.103317.
[68] B. Singh, G. Ishwarya, M. Gupta, S.K. Bhattacharyya, Geopolymer concrete: A review of some recent developments, Constr. Build. Mater. vol. 85 (2015) 78–90, https://doi.org/10.1016/j.conbuildmat.2015.03.036.
[69] X.S. Shi, F.G. Collins, X.L. Zhao, Q.Y. Wang, Mechanical properties and microstructure analysis of fly ash geopolymeric recycled concrete, J. Hazard Mater. vol. 237–238 (2012) 20–29, https://doi.org/10.1016/J.JHAZMAT.2012.07.070.
[70] A. Kumar Sinha, S. Talukdar, Mechanical and bond behaviour of high volume Ultrafine-slag blended fly ash based alkali activated concrete, Constr. Build. Mater. vol. 383 (2023) 131368, https://doi.org/10.1016/J.CONBUILDMAT.2023.131368.
[71] Y. Patrisia, D.W. Law, C. Gunasekara, A. Wardhono, Life cycle assessment of alkali-activated concretes under marine exposure in an Australian context, Environ. Impact Assess. Rev. vol. 96 (2022) 106813, https://doi.org/10.1016/J.EIAR.2022.106813.
[72] L. Nguyen, A.J. Moseson, Y. Farnam, S. Spatari, Effects of composition and transportation logistics on environmental, energy and cost metrics for the production of alternative cementitious binders, J. Clean. Prod. vol. 185 (2018) 628–645, https://doi.org/10.1016/J.JCLEPRO.2018.02.247.
[73] K.K. Ramagiri, A. Kar, Environmental impact assessment of alkali-activated mortar with waste precursors and activators, J. Build. Eng. vol. 44 (2021) 103391, https://doi.org/10.1016/J.JOBE.2021.103391.